Supplementary Materials for

A Mobile Robotic Process Chemist

Emma J. Brass, Satheeshkumar Veeramani, Zhengxue Zhou, Hatem Fakhruldeen, J. Sebastian Manzano, Rob Clowes, Isil Akpinar, Miriam R. Ward, John W. Ward, Andrew I. Cooper

Corresponding author: aicooper@liverpool.ac.uk; john.ward@liverpool.ac.uk

The PDF file includes:

Materials and Methods
Supplementary Text
Figs. S1 to S39
Tables S1 to S4

Other Supplementary Materials for this manuscript include the following:

Movie S1
Movie S2

Supplimentary Discussion

Hardware components

Here we provide further information on the hardware used in the workflow.

OptiMax: We used an OptiMax 1001 from Mettler Toledo, configured with a 1000 mL reactor and an Alloy C-22 pitched-blade stirrer with four impellers at 60°. It has a temperature range of -40°C to 180°C. A touchscreen can be used for control of experimental parameters; the user can program a sequence of tasks and leave them to run unattended. The OptiMax can also be controlled via Mettler Toledo's proprietary iControl software on a connected computer. iControl provides more precise management of the experiment schedule and allows the user to control multiple pieces of Mettler Toledo equipment from one place. iControl has basic functionality for automation via XML files[35] or an OPC UA interface; neither of these provide a complete suite of functionality for building and running experiment files, and hence we used the Python library pywinauto[36] for GUI automation.

EasySampler: For sampling, we used a Mettler Toledo EasySampler 1210. A sampling probe sits in one of the OptiMax lid glass ports. A pocket extends out of the probe to take a 20 µL sample from the reaction mixture. This can be diluted from x80 to x450 in a solvent of choice connected to the EasySampler. In this work, we used a solution of 0.5 mg/mL caffeine in methanol as the dilution solvent (the caffeine being an internal standard for HPLC analysis). Samples were stored in 10 mL vials located on a vial carousel.

Syringe pump: Liquid reagent addition was carried out with a Tecan Cavro XLP 6000 syringe pump with a 12-port ceramic valve, PTFE tubing, and 25 mL syringe. The pump offers a high accuracy of ≤ 0.5% and a maximum flow rate of 50 mL/min.

Solid dispensing device: This bespoke solid dispensing device used in this work was designed to be compatible with a standard ISO ST29/32 ground glass joint. Because the device was 3D printed, it can be easily adapted to fit other ground glass joint sizes by editing the CAD files and reprinting. The device can hold a maximum of 30 g of 4-aminophenol, the solid reagent used in paracetamol synthesis, but it is more generally applicable to other solids. The weight of the device was 360 g. The cost of one solid dispensing device, including printer resin and electronic components, was £96 at current prices.

The solid-dispensing device consists of six parts printed in black photopolymer resin on a Formlabs 3+ SLA printer. The main cartridge is cylindrical and tapered at the end, to make it easier for the KUKA to maneuver the device into the ground glass joint port of the reactor. The cartridge has a side loading port, for the chemist to add solid into the cartridge, and handles for the robot arm gripper to grasp. Inside the cartridge is a shaft with a flat, half-circle base that keeps the cartridge closed. Above the main cartridge is casing for the motor. A push button is fixed into the casing, which can be operated by either a researcher or, in this workflow, the robot gripper.

Along with the solid addition device itself, we built a 3D printed ABS holder for the device to sit in when not being used. This was attached to the inside wall of the fume hood. Underneath the holder is an empty safety container. During normal operation this was not used, but it was designed to collect any powder leaks in the event of device breakage, which did not occur over the course of these experiments. Separately, there is a holder for an ST29/32 polypropylene stopper. The stopper has been modified with a 3D printed handle for the robot arm gripper to grasp. The stopper sits in a ground glass joint on the lid of the OptiMax when solid addition is not taking place.

The motor turns on when the button is pressed. This motor is connected to the spiral shaft, and hence the shaft rotates when the motor is on; this motion moves solid out of the bottom of the device. The power supply is a 6 V 3 A DC converter, plugged into a mains power socket. An alternative, battery-powered version of the device was created previously, but we switched to a mains power supply due to the limited battery lifetime and the need to run experiments continuously for extended periods of time.

When not in use, the cartridge sits in a holder attached to the wall of the fume hood. At a designated point in the reaction, the KUKA robot opens the fume hood door, manipulates the cartridge to add the solid, and then closes the fume hood door again and exits the area. The use of a mobile robot means that this low-cost solid addition device could be easily integrated into any fume hood, and could find applications beyond late-stage process chemistry (*e.g.*, for solid-state inorganic materials synthesis).

We performed tests to determine the accuracy of the solid dispensed from the device. These were performed by weighing approximately 20 g of 2-aminophenol into a glass beaker. The exact mass in the beaker was recorded to the nearest 0.01 g. Then the solid was poured into the cartridge through a powder funnel in the loading port. The cartridge was held over another empty beaker and the button was pressed manually to rotate the internal shaft. The mass of solid in this beaker was recorded to the nearest 0.01 g. The data are shown in Table S3. The mean mass loss in a dispense (that is, the quantity of solid that was not dispensed, because it remained in the dispenser) was 0.05 g, or 0.25%. Figure S1 shows the solid dispensing system in more detail.

Filtration and waste handling system: The filtration module sits directly underneath the base value of the OptiMax. It comprises a 900 mL glass crystallization dish with a 3D printed lid. The lid has a connection to vacuum and a connection to a peristaltic pump for waste drainage. The peristaltic pump moves waste filtrate to a 20 L HDPE container in the solvent cupboard below the fume hood. There is a conical depression in the filtration lid for a funnel to sit in. We lined the conical dip with a bespoke rubber cone made from Raytech Magic Rubber. Our funnels are 250 mL sintered glass funnels from Robu, porosity 3, with the stems cut off. When not in use, the funnels sit on a 3D printed shelving unit to the right of the OptiMax. During the workflow, the mobile robot moves the funnels around, gripping them by 3D printed handles fixed on the outside surface of the funnels. The handles are omnidirectional within the horizontal place; this

allows for flexibility in the direction of approach of the mobile robot gripper. The funnel handles have diagonal flanges above and below, which act as guides and allow for ±2 mm of error in the vertical position of the gripper.

Methods

Here we provide additional details on experimental setup, mobile robot configuration, and UHPLC-MS analysis methods.

Experimental setup: Prior to automated operation, the workflow required some manual preparation. Three clean sintered glass filtration funnels were placed on the shelves. The autosampler was fully loaded with clean 10 mL Mettler Toledo vials. The two solid dispensing cartridges were manually loaded with 20 g of 4-aminphenol each. To load them, the button was pushed until the internal shaft rotated to a position in which the bottom opening is covered. The lid was then taken off the loading port and replaced with a powder funnel. 20 g of 4-aminophenol was transferred into the cartridge, and the loading port lid was replaced. The cartridge was placed in its holder and power cables were connected.

Manual experiment: We performed an analogous manual synthesis of paracetamol, to compare yields with the automated experiments. This manual synthesis was carried out in the same fume hood as the automated runs. The chemist measured out 450 mL of distilled water and poured this into the OptiMax via one its ports. The chemist then weighed out 20 g of 4-aminophenol into a beaker and added this into the OptiMax, using another 50 mL of distilled water to wash out residual 4-aminophenol. The reactor was operated, using the iControl touchscreen interface, to heat the mixture to 70 °C. The EasySampler was also operated using the same touchscreen; the chemist used it to take a 20 µL sample. After the first sample, 35 mL of acetic anhydride was weighed out an poured into the reactor. The chemist manually transferred the sample to the UHPLC-MS machine and ran the sample via the MassLynx software interface. Samples were taken until the sample concentration was above 0.45 mg/mL. Then, the chemist used to touchscreen interface to cool the reactor to 5 °C over 30 min.

The chemist set up a Buchner funnel filtration. The OptiMax base valve was opened by sending the appropriate serial command to the base valve Arduino; the base valve automation setup cannot be easily removed, so we left it on for the manual reaction. The slurry from the OptiMax was collected in a large beaker and then filtered under vacuum. After being left to dry under vacuum for 5 minutes, the product was weighed.

To clean the reactor, 600 mL of distilled water was added and it was heated to 85 °C. Again, a sample was transferred to the UHPLC-MS for analysis. The reactor was drained and refilled, and a sample was taken, until the paracetamol concentration in the sample was below 0.05 mg/mL and two cleaning cycles were completed.

The reaction scheme is shown below.

$$H_2NC_6H_4OH + (CH_3CO)_2O \longrightarrow HOC_6H_4NHCOCH_3 + CH_3COOH$$

Mobile robot: The mobile robot was a KUKA KMR iiwa. It navigated using LiDAR sensors with simultaneous localization and mapping (SLAM) algorithms to pinpoint its location on a map of the laboratory environment (Figure S2). The base had a positioning accuracy of ±5mm. The mobile base has a payload of 200 kg and the robot arm has a payload of 14 kg.

We introduced an advanced vision-based calibration system, surpassing our previous tactile-based method in both efficiency and adaptability. The integration of the vision server within our automated framework employs a client-server architecture, which provided real-time marker poses to the robot. These poses were used for calibrating the robot's end-effector in relation to the objects it manipulates. On the client side, a Java-based package, deployed directly on the KUKA robot's control unit, facilitates seamless interaction between the robot and the vision server. This configuration allows the robot to dynamically adjust its operations based on immediate feedback from the vision server, thereby ensuring sustained precision and reliability throughout the experimental workflow.

Central to this system was a robust edge-computing server powered by Nvidia Jetson Xavier NX, which processed high-resolution images (1920 x 1080 pixels) of the main calibration boards, each measuring 75 mm by 75 mm. To thoroughly evaluate the system's repeatability and endurance, we conducted extensive testing using a smaller 20 mm x 20 mm calibration board. This board was tested over a duration of 8 hours, which included 600 pickup and insertion manipulations, thereby validating the system's operational reliability and effectiveness under prolonged operational conditions without fail.

To ensure the mobile robot remained operational throughout the workflow, two maintenance tasks needed to be performed alongside the main workflow tasks: autocalibration and auto-charging. The autocalibration task helps to maintain the accuracy and precision of the robot arm's manipulation, while the auto-charging task ensures the battery of the robot does not drop below the minimum required level. Individual state machines on the robot controller continuously monitor the elapsed time since the previous calibration and the current battery level for autocalibration and auto-charging, respectively. When the elapsed time exceeded a predefined limit, the autocalibration process commanded the mobile robot to navigate to a safe location and perform the arm-referencing task; this calibrated the encoders of all joints. When the robot's battery level fell below a predefined lower limit, the auto-charging process commanded the robot to navigate to the docking position on a charging plate embedded into the laboratory floor. The charging process then began and continued until the battery level reached the predefined upper limit. Once charging was complete, the robot either began the first task in the workflow buffer straightaway or navigated to a safe location to await the next task.

Maintenance tasks were given higher priority. Workflow tasks accumulated in a buffer while the robot was in charging or calibration states. Once these states were completed, the robot started performing the workflow tasks sequentially. Similarly, when the robot received a maintenance call while executing a workflow task, it completed the current task and then proceeded to maintenance, even if other workflow tasks remained in the buffer.

UHPLC-MS analysis and decision making: The UPLC-MS measurements were performed using a Waters Acquity UPLC-MS. The machine was equipped with an Automation Portal attachment to allow for robotic placement of samples. Samples were run using water and acetonitrile as the mobile phase. Liquid chromatography was performed on an Acquity UHPLC BEH C18 column. The gradient profile is shown in Figure S5.

To allow for the Mettler Toledo 10 mL sample vials to be run on the Waters UHPLC-MS, we designed a custom vial rack to fit in the UHPLC-MS (Figure S6). We used 3D printing to create initial prototypes, then the finalized design was milled externally in acetal plastic. We created a custom profile for this rack within the Waters MassLynx software. The Mettler Toledo 10 mL vials came with non-slit 1.5mm thick septa; these were too thick for use in our UHPLC-MS machine. We replaced them with pre-slit 1mm thick septa.

We looked only at the paracetamol concentration within each sample. The 4-aminophenol concentration could be misleading particularly at the beginning of the experiment, as the compound was added as a solid and hence most of it is not in solution when the first sample is taken. The samples were made up in 0.5 mg/mL solution of caffeine in MeOH; caffeine served as an internal standard. The concentration of paracetamol within the sample was calculated using calibration curves, created from comparing the peak area ratio (peak area of compound of interest vs. peak area of caffeine) to the real concentration of the compound of interest.

The labmatic package consisted of a client that sits on the computer running ARChemist, and a server that sat on the PC running the Waters MassLynx software. The client sent the server a CSV file via a socket connection, which detailed the methods to be run on each sample. This triggered startup of the UHPLC-MS and analysis of the sample. The output RAW file was analyzed by the client and compound concentration data is sent back to the server. The labmatic package used the photo diode array (PDA) data at 210-400 nm. Baseline estimation was performed using an asymmetric least squares method.[37] Peak areas were calculated using the trapezoidal method with the trapz() function in numpy. The retention times for 4-aminophenol and paracetamol were known beforehand. During experiments, labmatic assigned a compound identity to a peak with a maxima within ±0.1 min of the expected retention time for that compound. If there were multiple peaks within the range, an error was thrown.

A 100% yield as determined by UHPLC-MS analysis would correspond to a sample paracetamol concentration of 0.528 mg/mL. A concentration of 0.45 mg/mL, corresponding to a yield of 87% before workup, was chosen as the target yield, whereupon the system was ready to move on to workup steps. In the cleaning stages, a concentration of 0.05 mg/mL was chosen as a threshold below which the cleaning is considered complete. The system was set to do at least two

cleaning cycles, even if the paracetamol concentration was below the threshold in the first cleaning sample, to ensure cleanliness of the reactor.

Data on the paracetamol peak areas vs caffeine peak areas for the sample taken after acetic anhydride addition for each experiment is shown in Table S4.

Experiments reported in main paper

In Table S1, we report the yield outputs from three successive experiments carried out on August 28th 2024. The experiments on August 28th 2024 obtained an average yield of 56.9 ± 0.1%.

Preliminary experiments

Prior to the experiments reported above (August 28th 2024), we carried out several trial experiments that failed due to errors. Yield outputs are shown in Table S2. To give a sense of the platform development, and the types of errors encountered and their resolution, we give brief details of some of those preliminary experiments below.

Experiments Jan 17th, 2024: Here we ran two successive syntheses. The first experiment was completed fully, but the second experiment failed during filtration. This is because the seal between the filtration funnel and the rubber cone broke, allowing air to be drawn in around the funnel instead of through it. Consequently, the funnel to overflowed with liquid. This was fixed by making a bespoke rubber cone out of RayTech Magic Rubber and adding a step where the robot gripper presses down on the funnel after placement. Sample UHPLC-MS data is shown in Figures S8-S13.

Experiments Jan 18th, 2024: The first experiment was completed fully. In the second experiment, the sample concentration after the second sample was 0.4359, corresponding to a yield of 83%, below the threshold of 87%. We manually intervened via the software and moved the workflow on, to continue testing and looking for errors. The workflow then failed after weighing but before UHPLC-MS analysis of the first cleaning sample. The robot dropped the first cleaning sample while removing it from the fume hood. We solved this by adding a thin layer of rubber to the inside surface of the fingertips, to prevent slippage. Sample UHPLC-MS data is shown in Figures S14-S19.

Experiments August 5th, 2024: The first experiment failed after weighing but before the first cleaning sample. This was due to an error in the frame coordinates for robot movement and was solved by correcting the coordinates. Sample UHPLC-MS data is shown in Figures S20-S21.

Experiments August 8th, 2024: The first experiment was completed successfully, but the second experiment failed after filtration but before weighing. This was again due to an error in frame coordinates for robot movement. Sample UHPLC-MS data is shown in Figures S22-S27.

Workflow limitations and future refinements

The workflow currently only employs two solid dispensing devices. For the paracetamol experiments, this means the solid dispensing devices must be manually reloaded approximately every 14 hours. The reload rate could be easily improved by adding more solid dispensing devices into the fume hood.

Looking at the paracetamol concentrations shown in Table S3 for the samples taken after acetic anhydride addition, we see that the concentrations were all above 0.45 mg/mL (87%), excluding the January 18th experiment discussed previously, and in most cases near the 0.538 mg/mL required for a 100% yield. However, the final isolated gravimetric yields were closer to 55%. The lower final yields were due incomplete product crystallisation and, to a lesser extent, product being washed out during the wash step in filtration. This was not an error of the automated system *per se* since essentially the same yields were achieved when a human researcher followed the same protocols. Future work could look to improve the yields by first increasing the crystallisation cooling time, for example.

Safety note

The implementation of experiments that operate overnight in an automated way must be carefully risk assessed, particularly when using new technologies. As reaction scales increase, as in late-stage process chemistry, this becomes even more important. We adopted the following basic principles in developing this workflow.

- Start with relatively low hazard chemistry. Paracetamol synthesis is well known, and the synthesis route uses water as a solvent.
- Do not operate systems overnight until there is a high level of confidence in the automated methods. All reactions were carried out in an operator-supervised fashion prior to this and we carried out multiple trial runs over a period of a year before carrying out the three back-to-back reactions exemplified in Movie S2.
- Use of multiple CCTV cameras to record activity in the laboratory and diagnose problems. These cameras can also be accessed remotely.

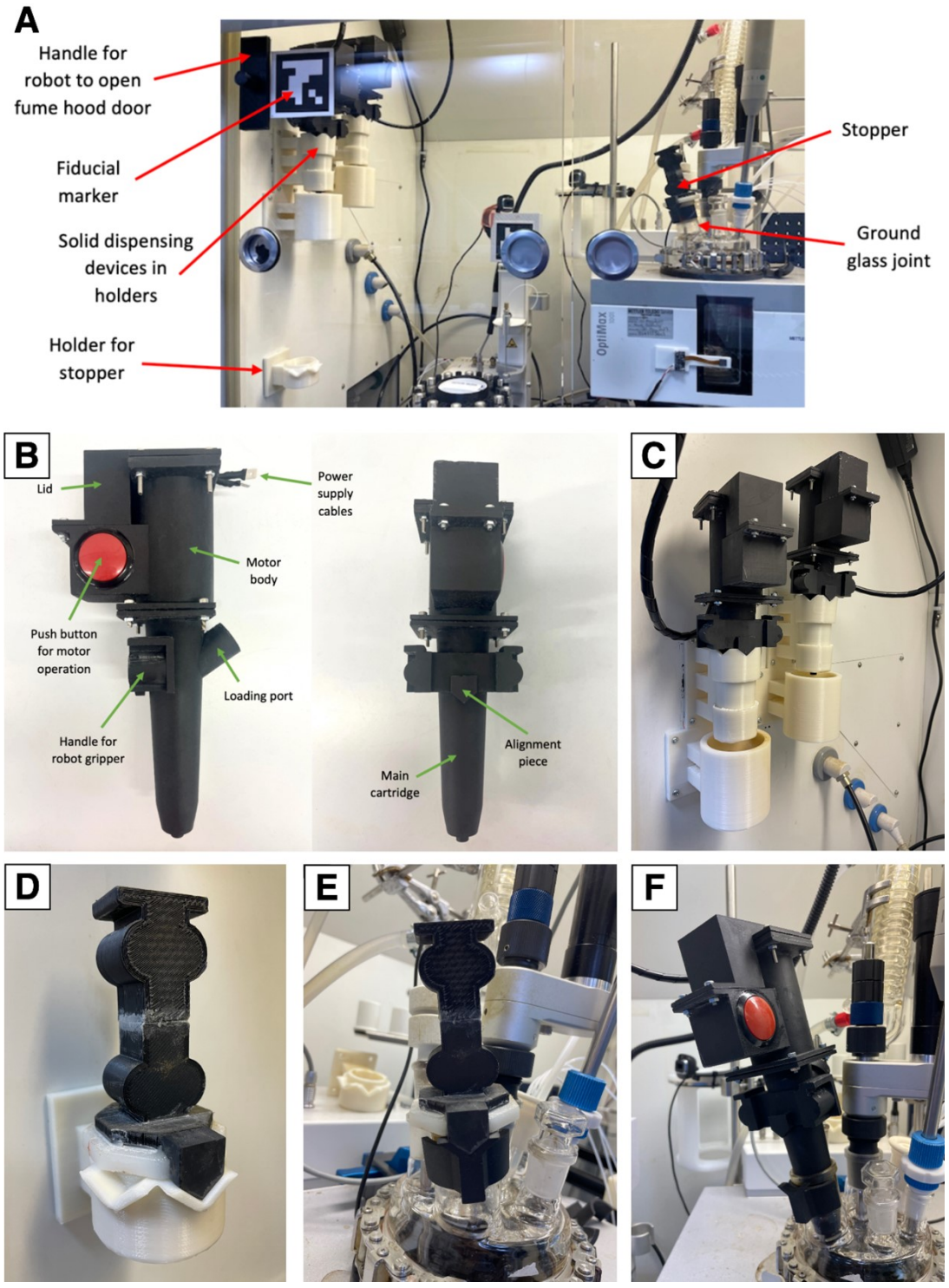

Fig. S1.

(**A**) The solid dispensing device setup in the fume hood. (**B**) Labelled components of the device, shown from the side (left) and from the back (right). (**C**) The two solid dispensing devices in

their holders on the fume hood wall. (**D**) The stopper in its holder on the fume hood wall. (**E**) The stopper in the reactor port. (**F**) The solid dispensing device sitting in the reactor port.

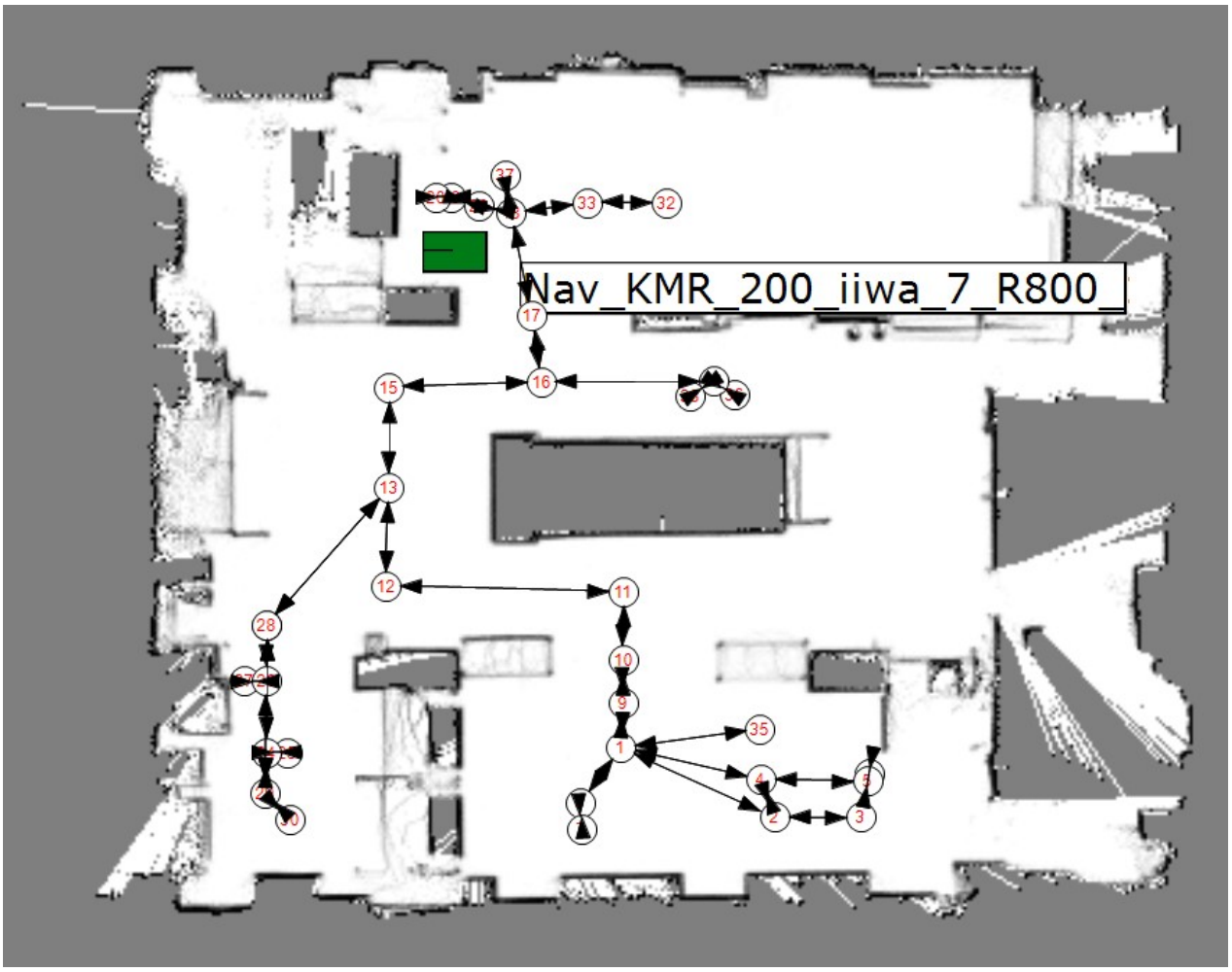

Fig. S2.

The LIDAR map of the laboratory used by the mobile robot for navigation, showing pre-saved waypoints (numbered circles).

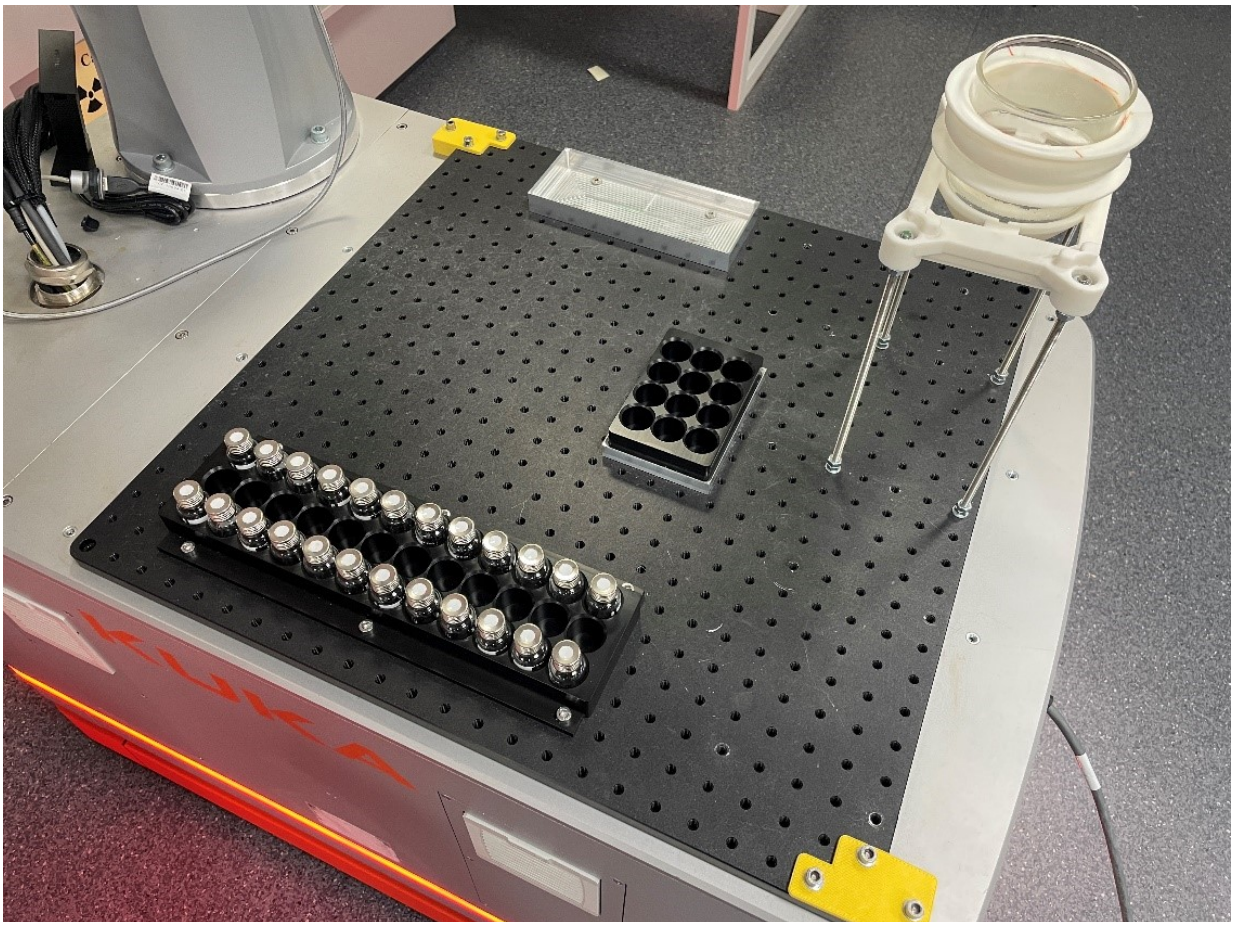

Fig. S3.

The base of the mobile robot, equipped with a long rack for storing used samples, a short rack for the sample being transported, and a raised holder for a hollow funnel that is used during cleaning.

Fig. S4.

The end effector used by the mobile robot. The gripper is an OnRobot RG6 Gripper, and the fingertips were custom designed in-house and printed in resin. The camera is an Intel RealSense Depth Camera D435i.

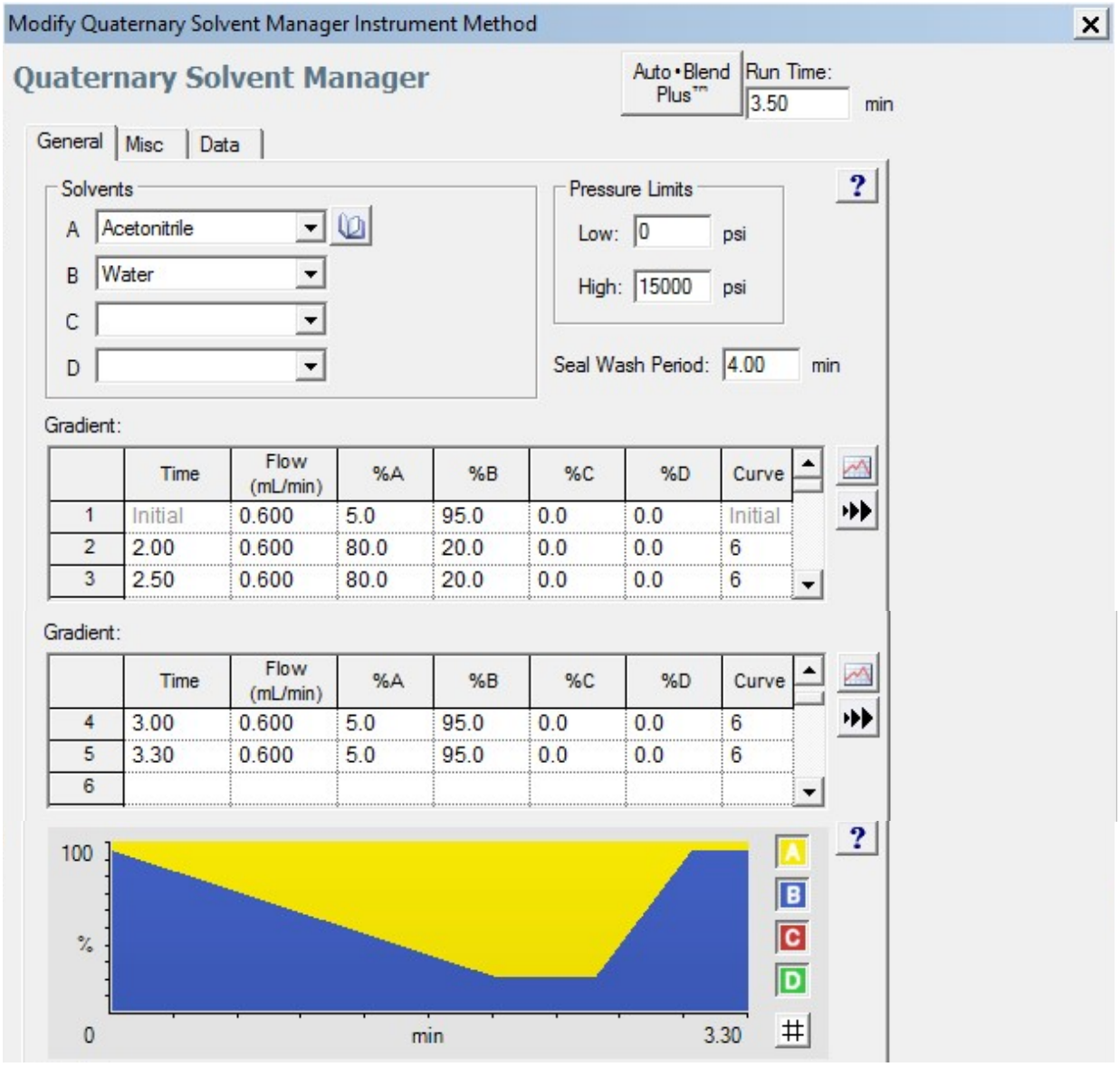

Fig. S5.

Gradient profile for the Waters UHPLC-MS.

Fig. S6.

The custom vial rack designed to holder Mettler Toledo 10 mL vials and fit in the Waters UHPLC-MS machine.

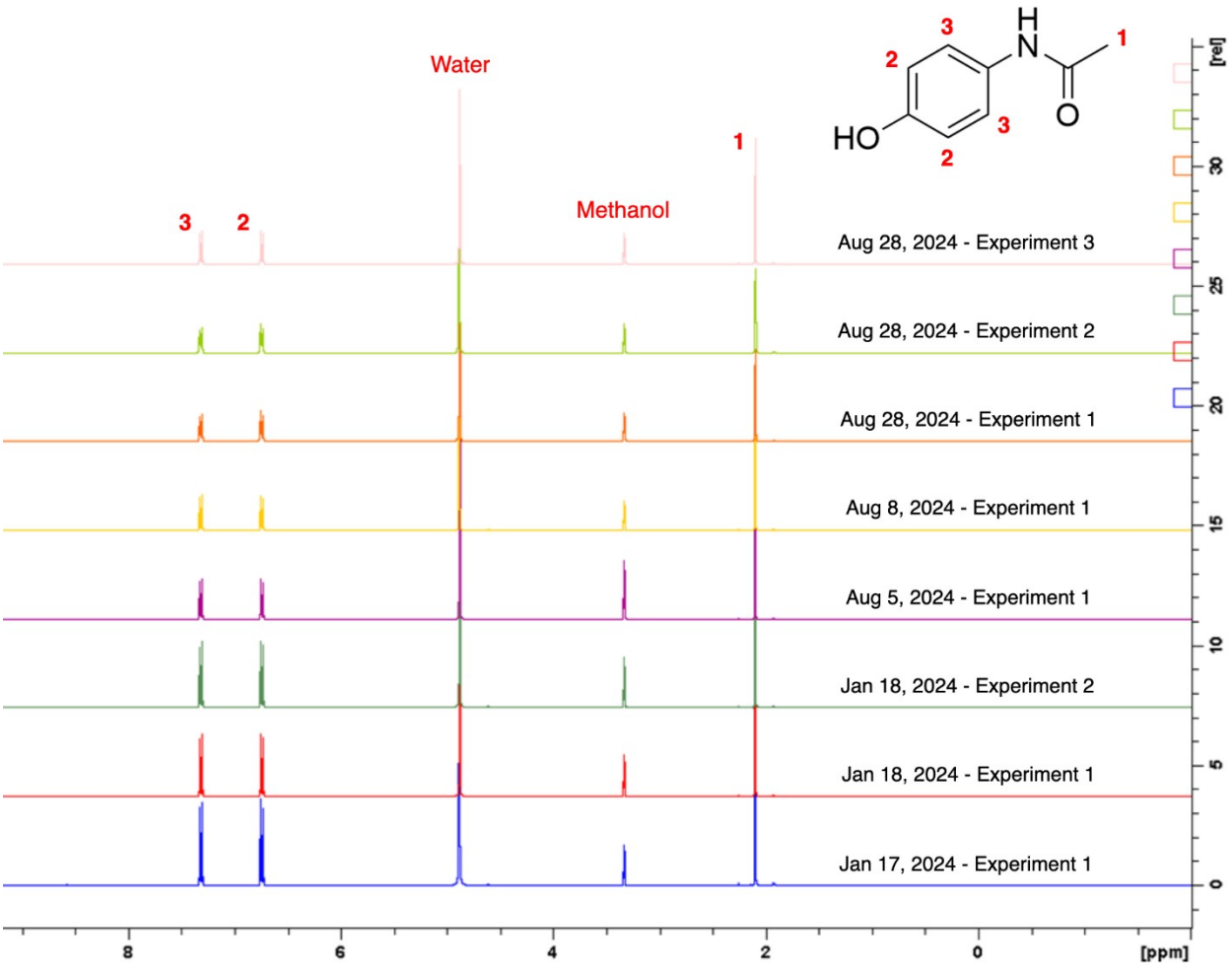

Fig. S7.

NMR data from eight automated paracetamol synthesis experiments. Solvent is methanol-d4.

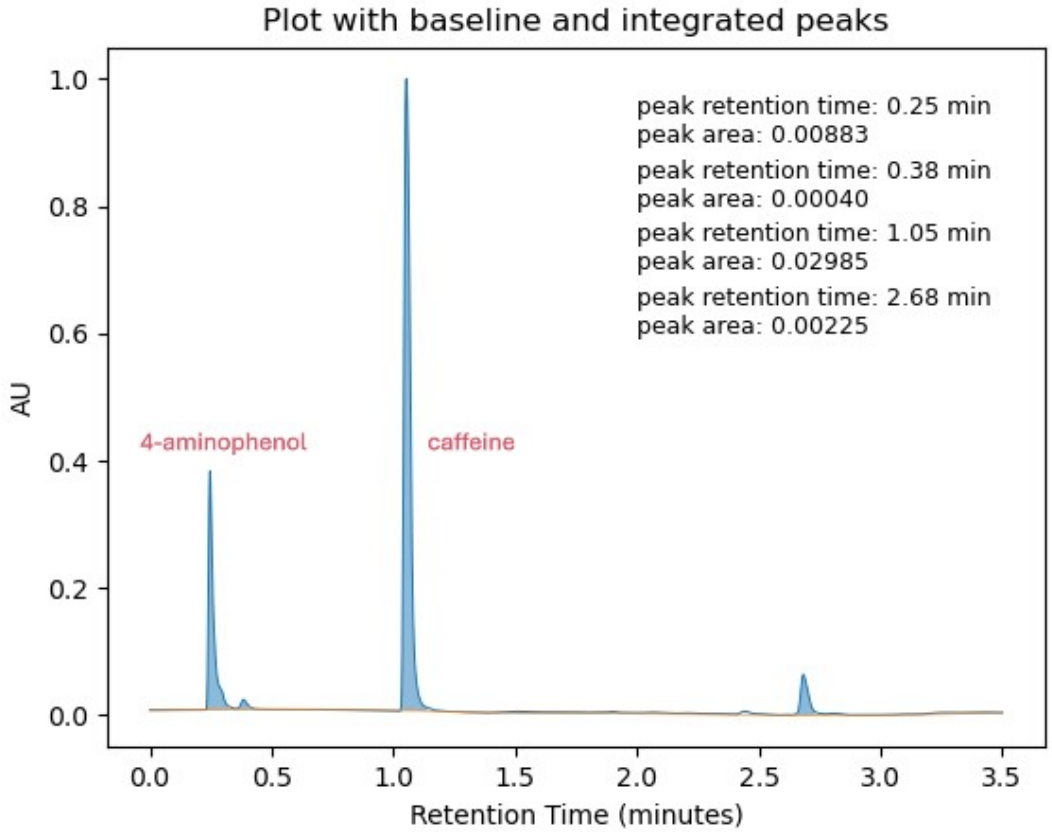

Fig. S8.

17/01/2024 - 17:00:08 – Experiment 1 – Before acetic anhydride addition. We note the presence of small impurity peaks in the UHPLC data at ~ 2.7 min. The identity of this compound is unknown; we saw no extra peaks in the NMR samples.

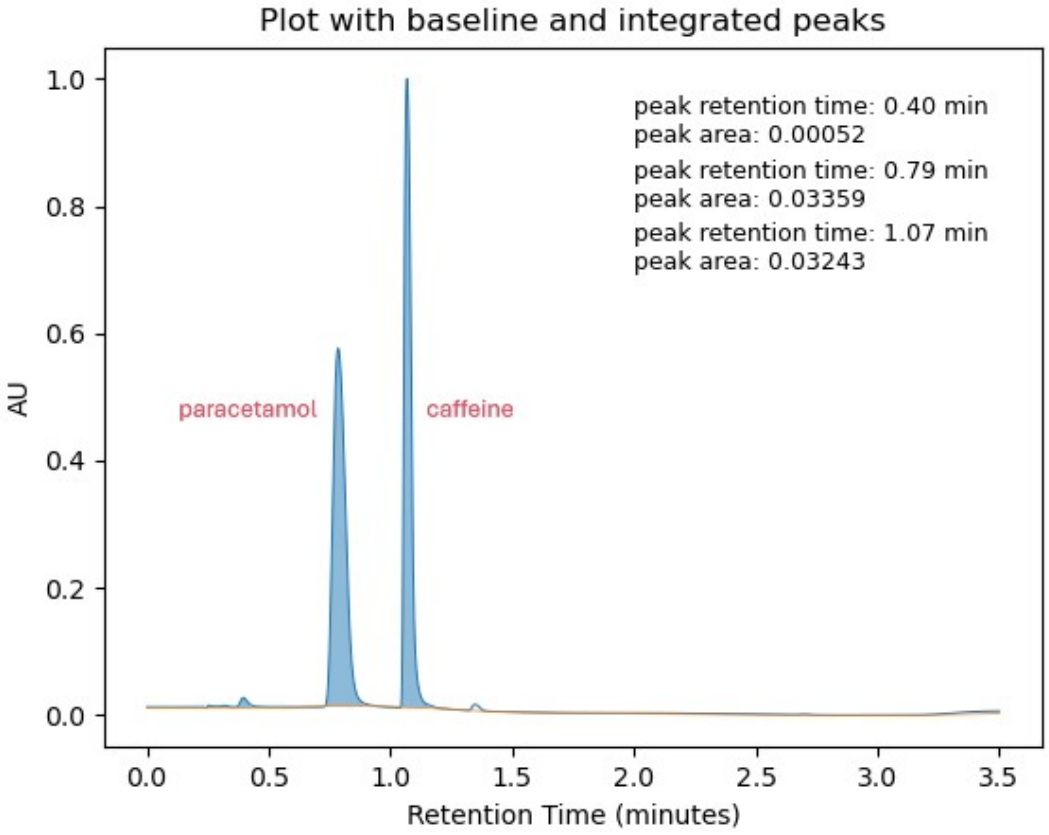

Fig. S9.

17/01/2024 - 17:34:19 – Experiment 1 – After acetic anhydride addition

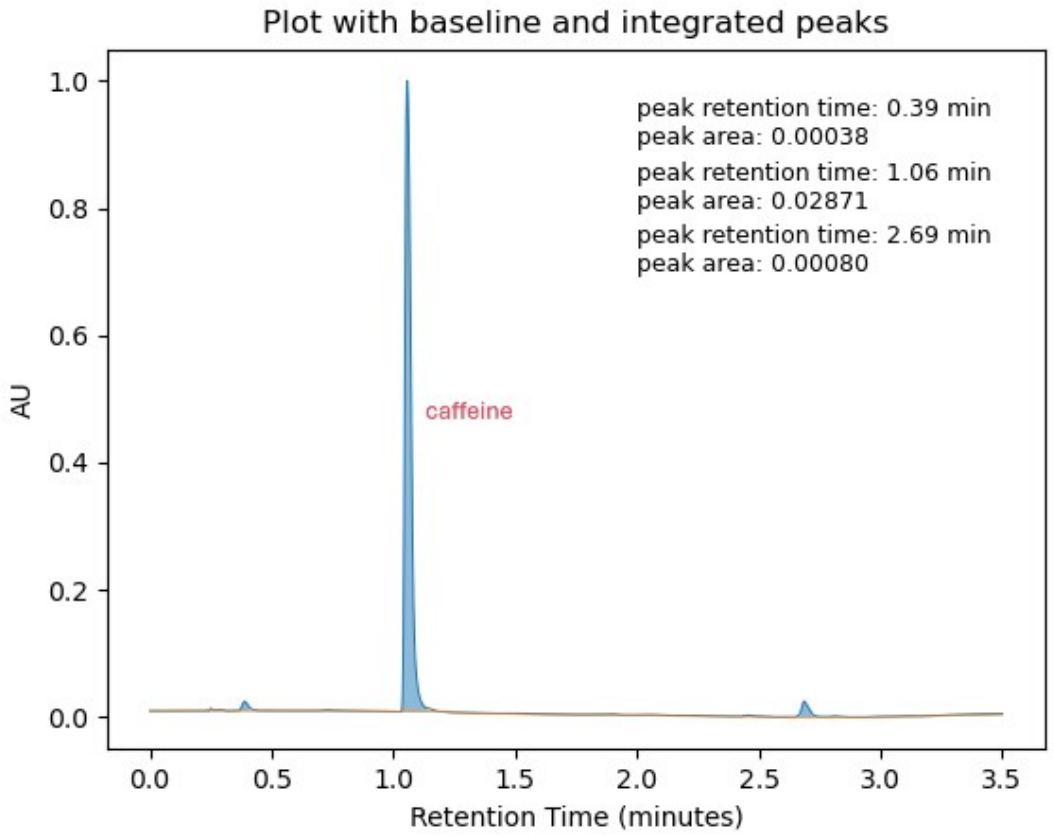

Fig. S10.

17/01/2024 - 20:11:52 – Experiment 1 – Cleaning sample 1

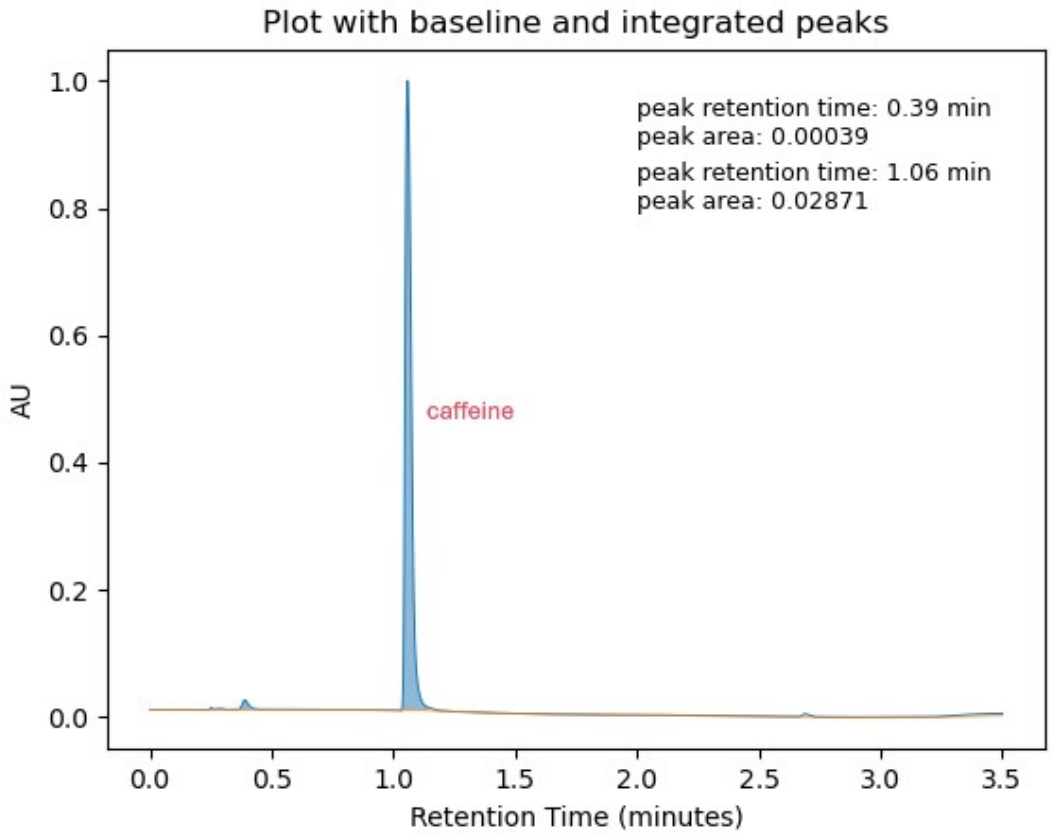

Fig. S11.

17/01/2024 - 21:04:39 – Experiment 1 – Cleaning sample 2

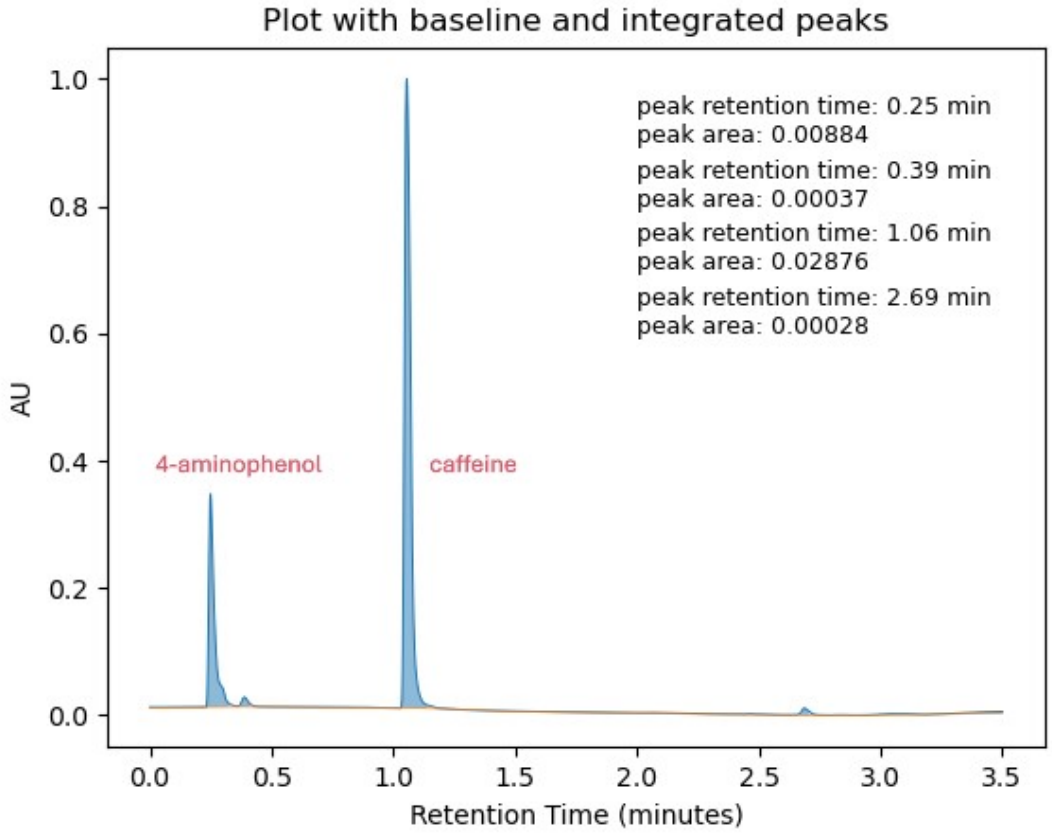

Fig. S12.

17/01/2024 - 22:29:32 – Experiment 2 – Before acetic anhydride addition

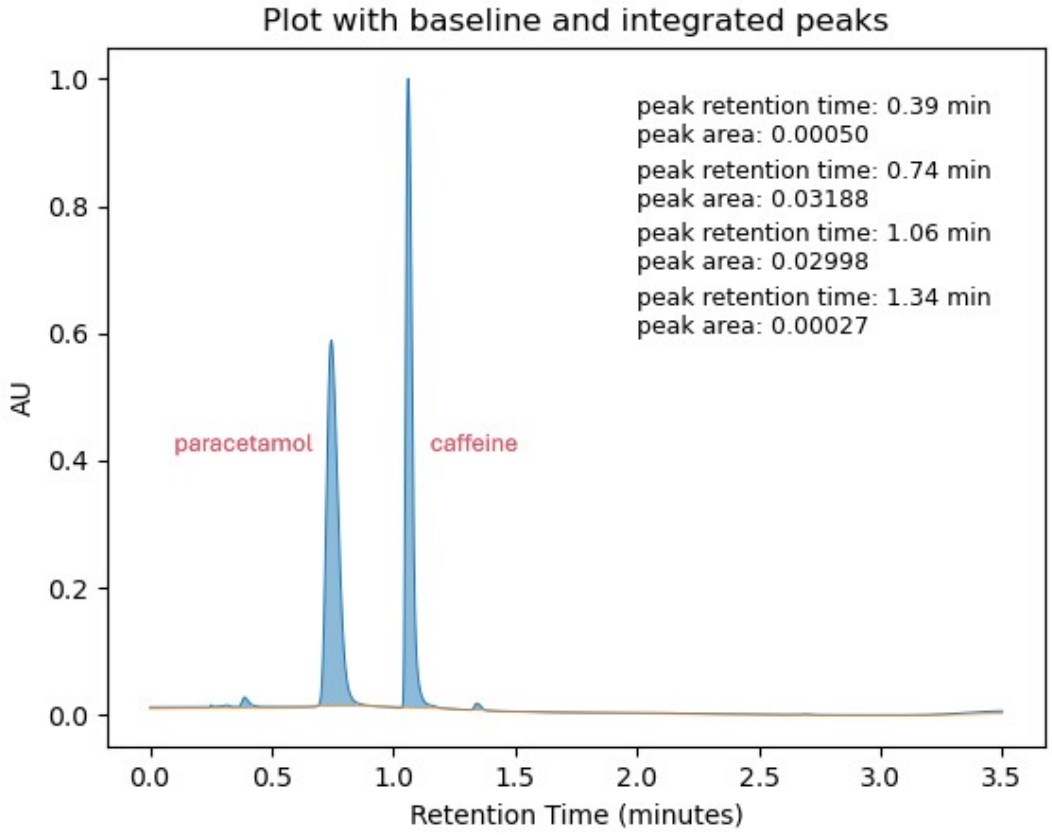

Fig. S13.

17/01/2024 - 23:05:18 – Experiment 2 – After acetic anhydride addition

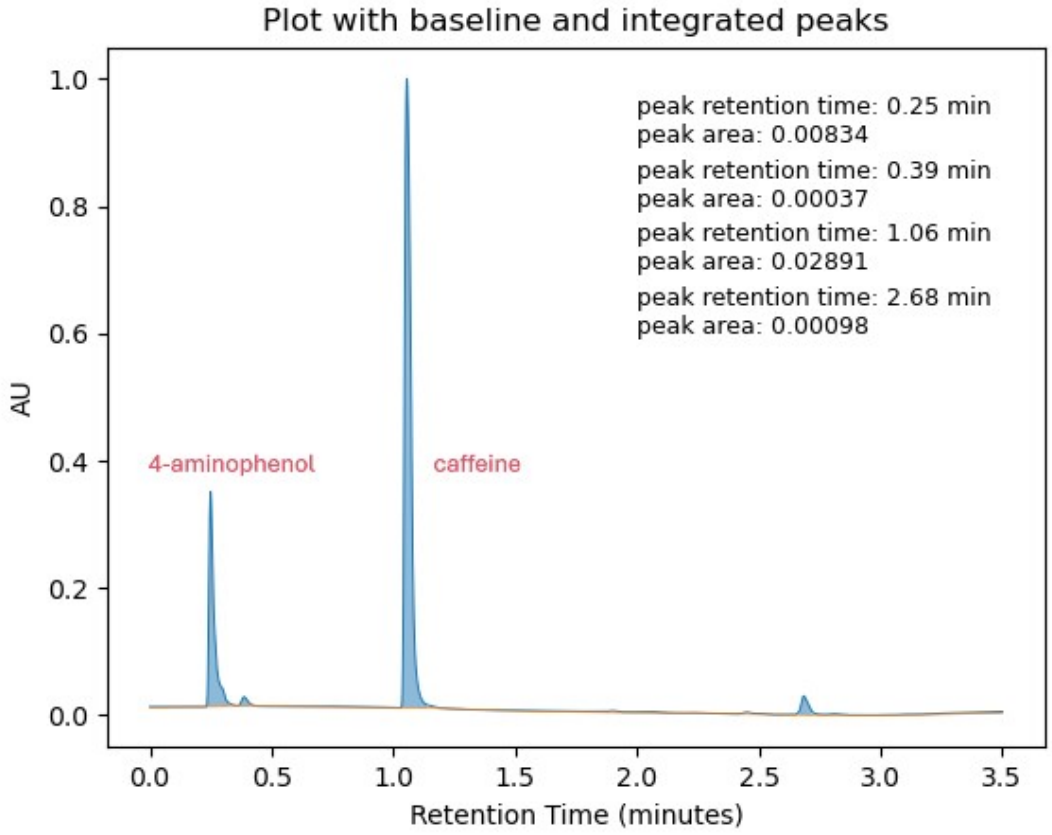

Fig. S14.

18/01/2024 - 11:34:18 – Experiment 1 – Before acetic anhydride addition

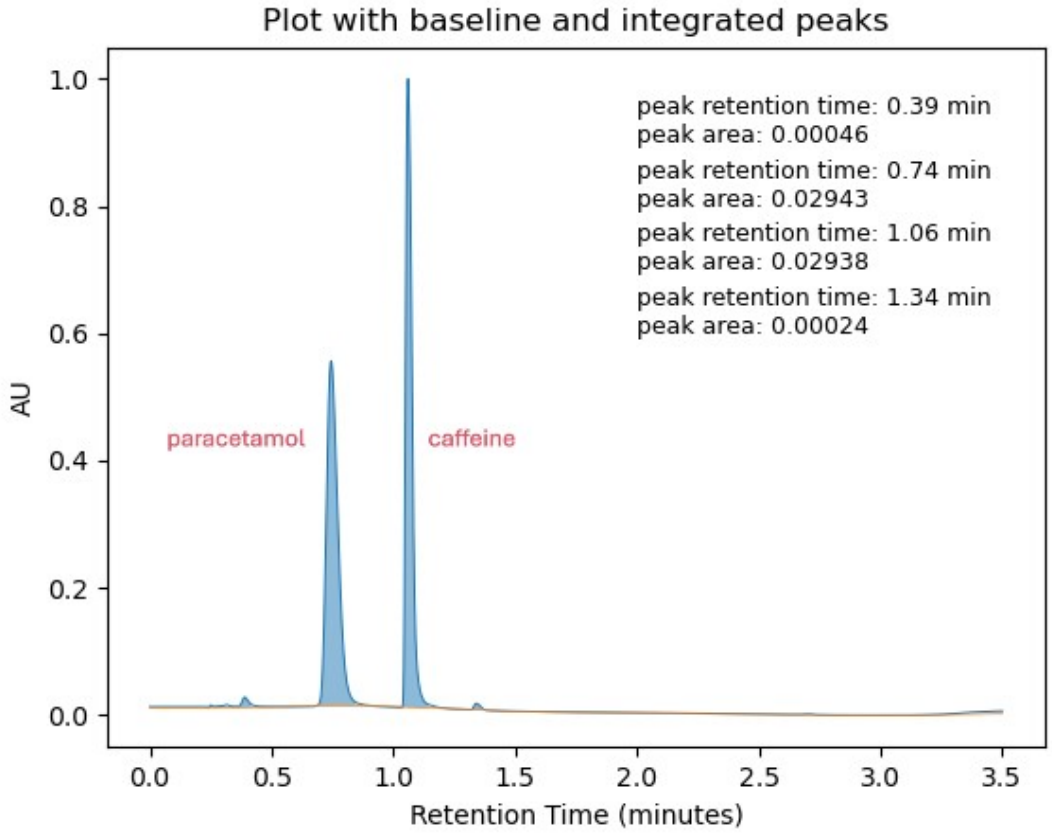

Fig. S15.

18/01/2024 - 12:11:08 – Experiment 1 – After acetic anhydride addition

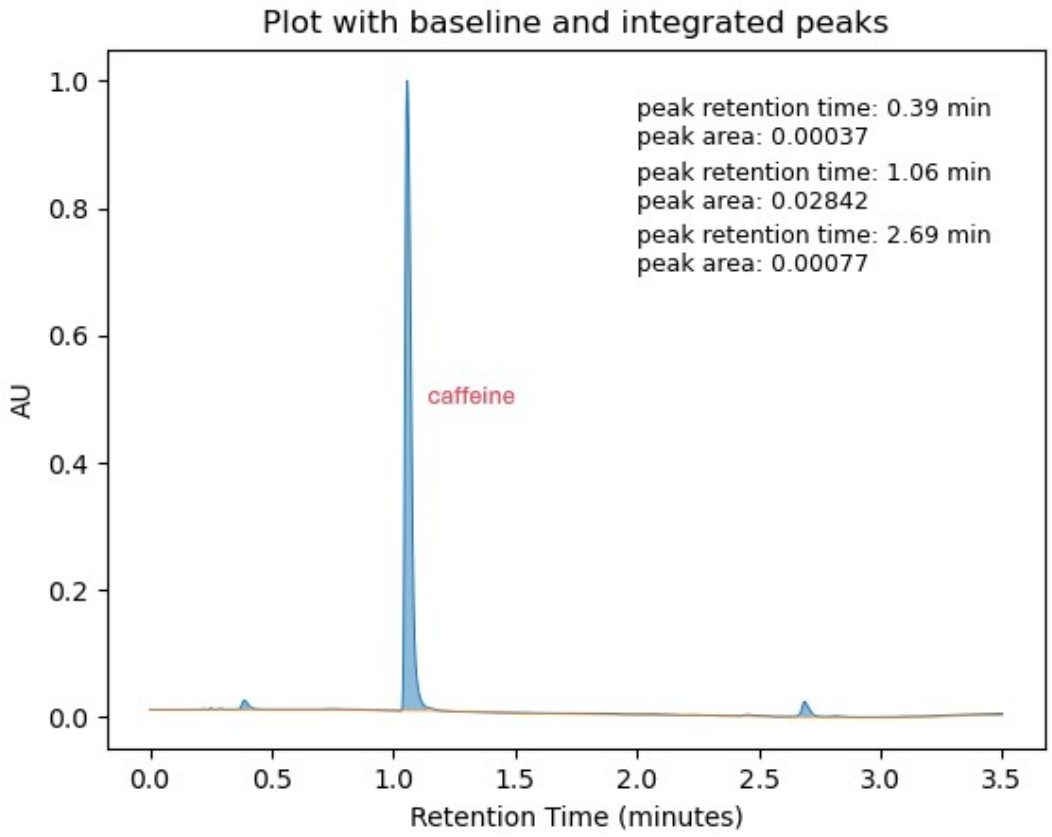

Fig. S16.

18/01/2024 - 14:46:47 – Experiment 1 – Cleaning sample 1

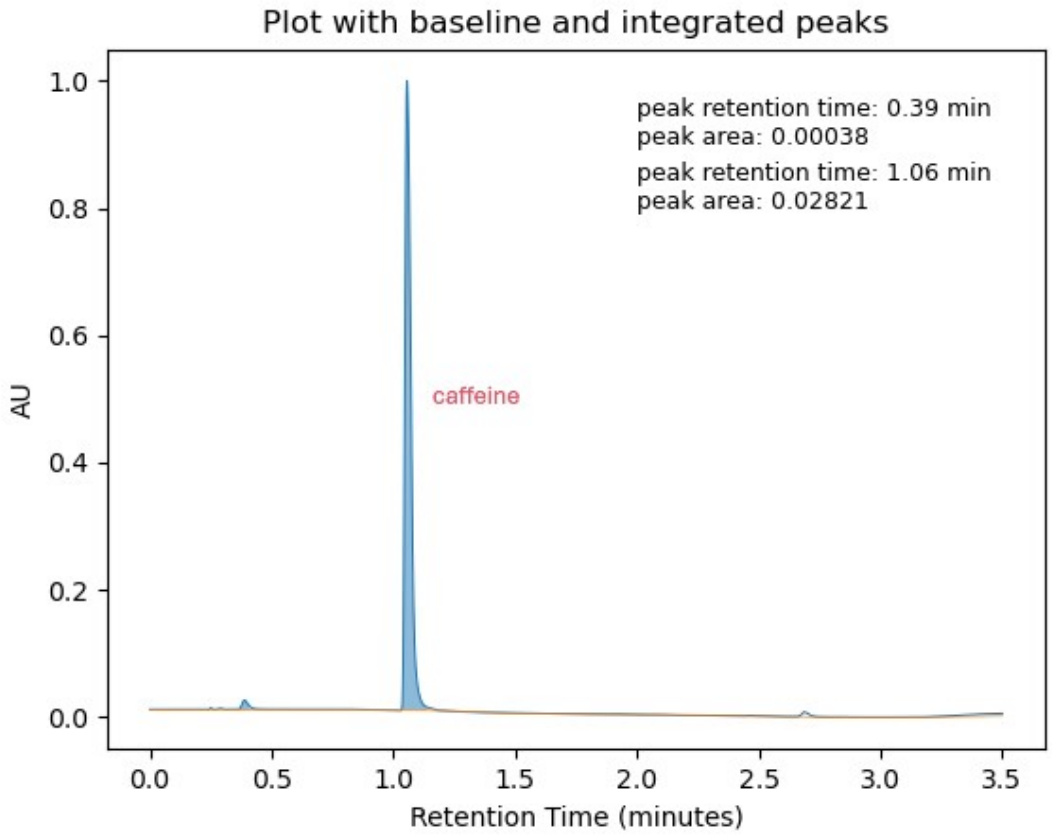

Fig. S17.

18/01/2024 - 15:56:04 – Experiment 1 – Cleaning sample 2

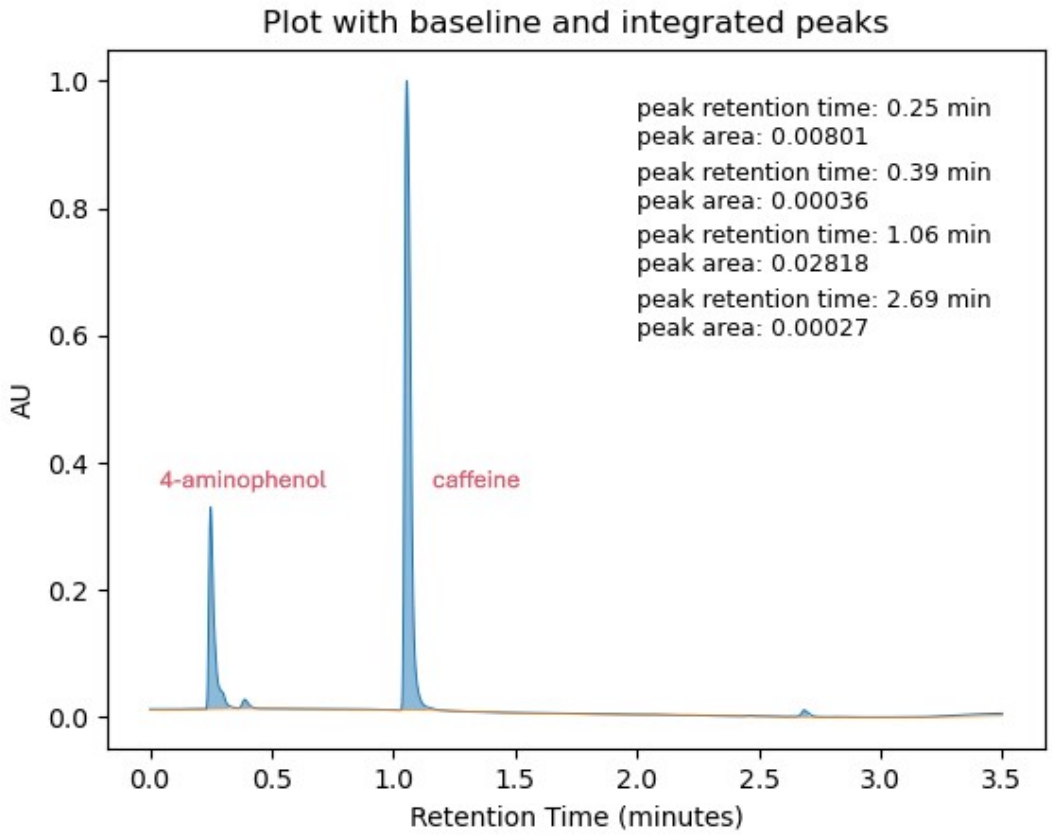

Fig. S18.

18/01/2024 - 17:21:18 – Experiment 2 – Before acetic anhydride addition

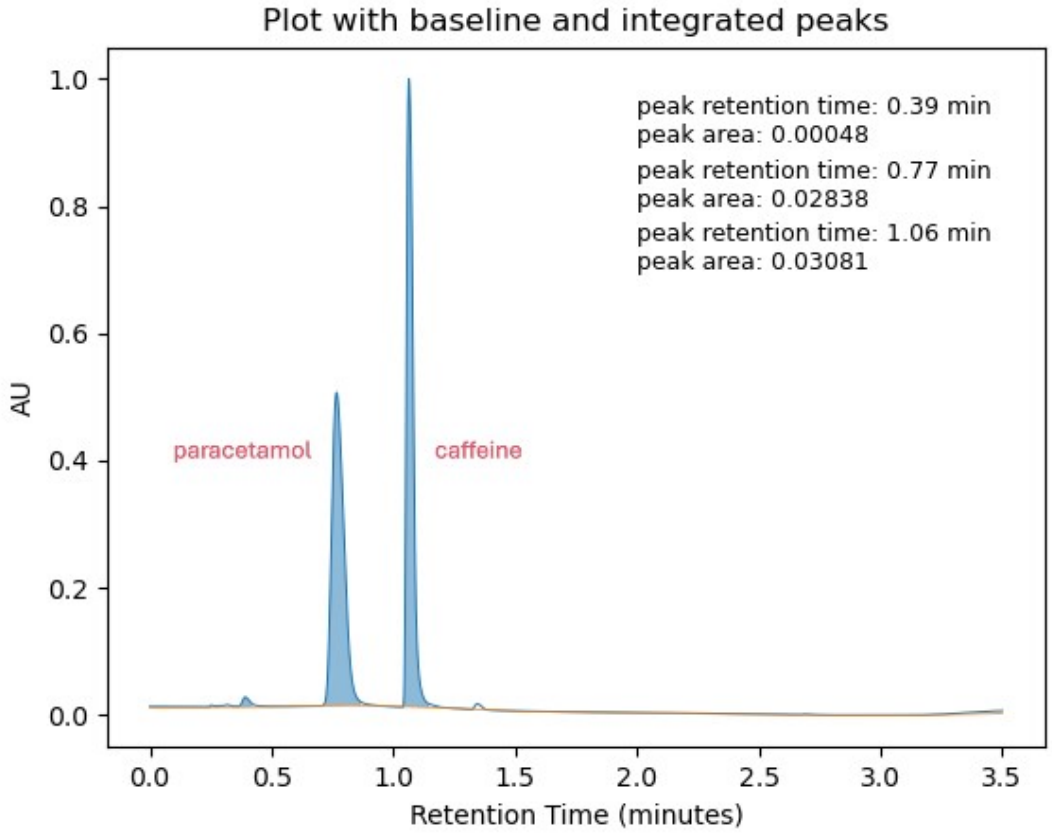

Fig. S19.

18/01/2024 - 17:55:59 – Experiment 2 – After acetic anhydride addition

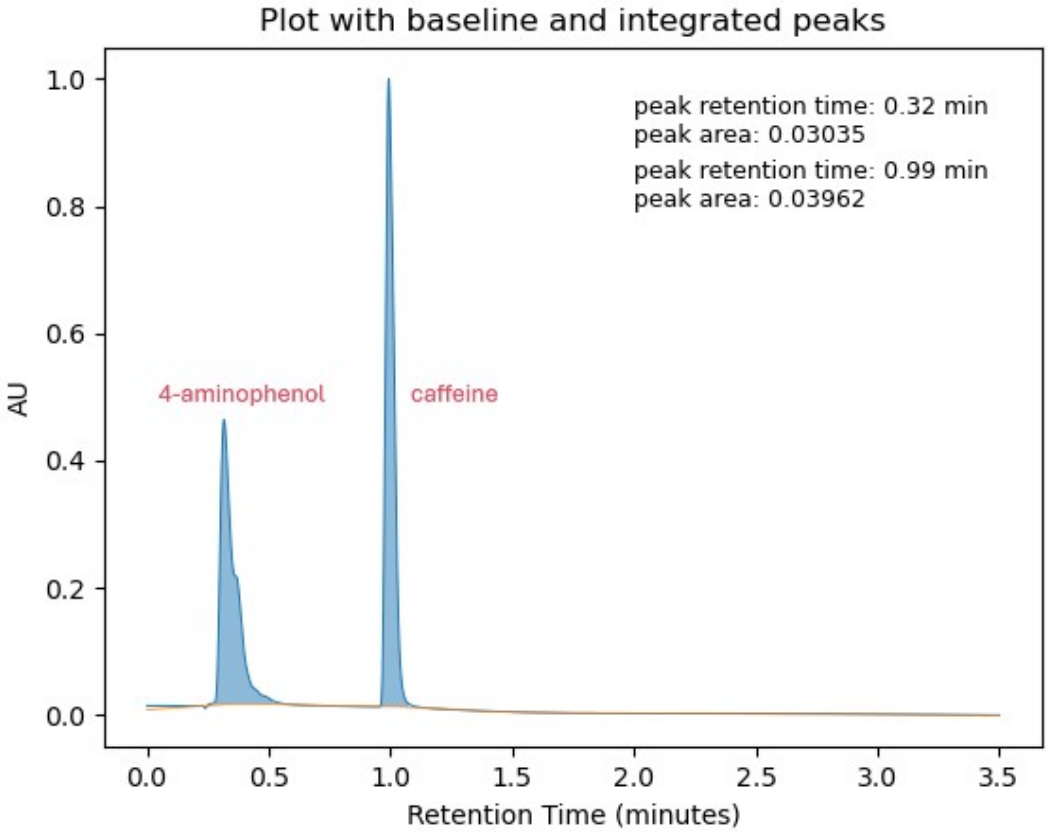

Fig. S20.

05/08/2024 - 18:33:46 – Experiment 1 – Before acetic anhydride addition

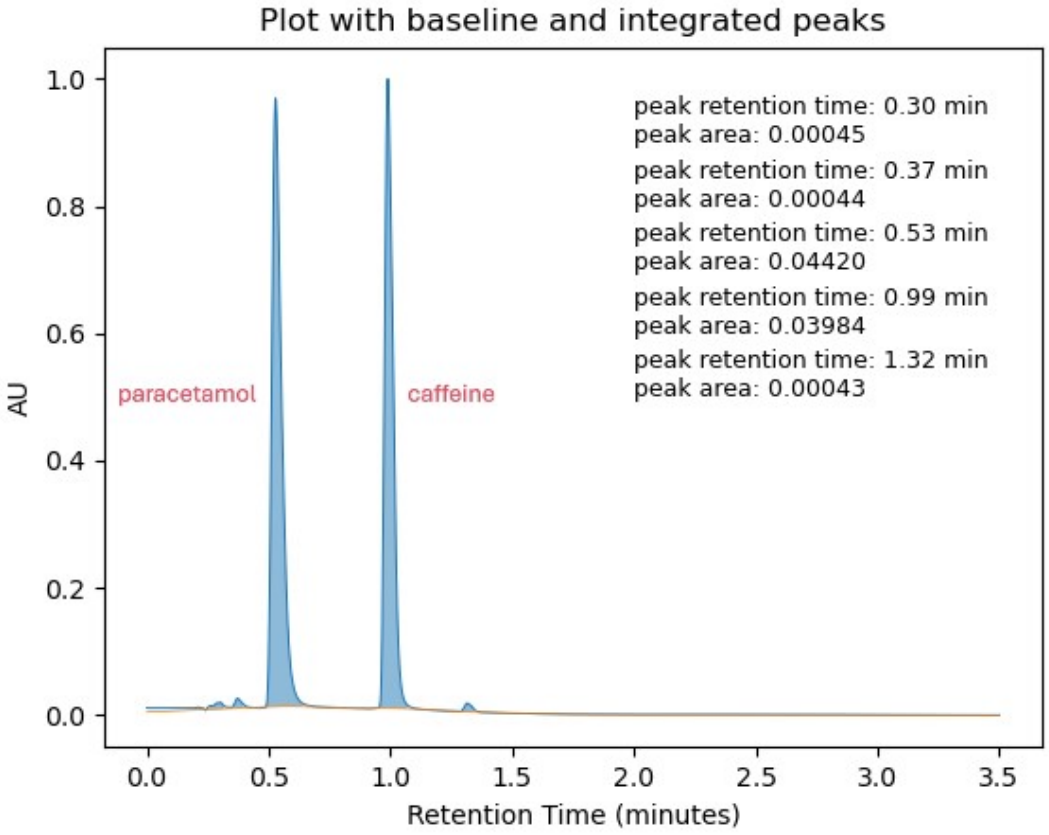

Fig. S21.

05/08/2024 - 19:21:19 – Experiment 1 – After acetic anhydride addition

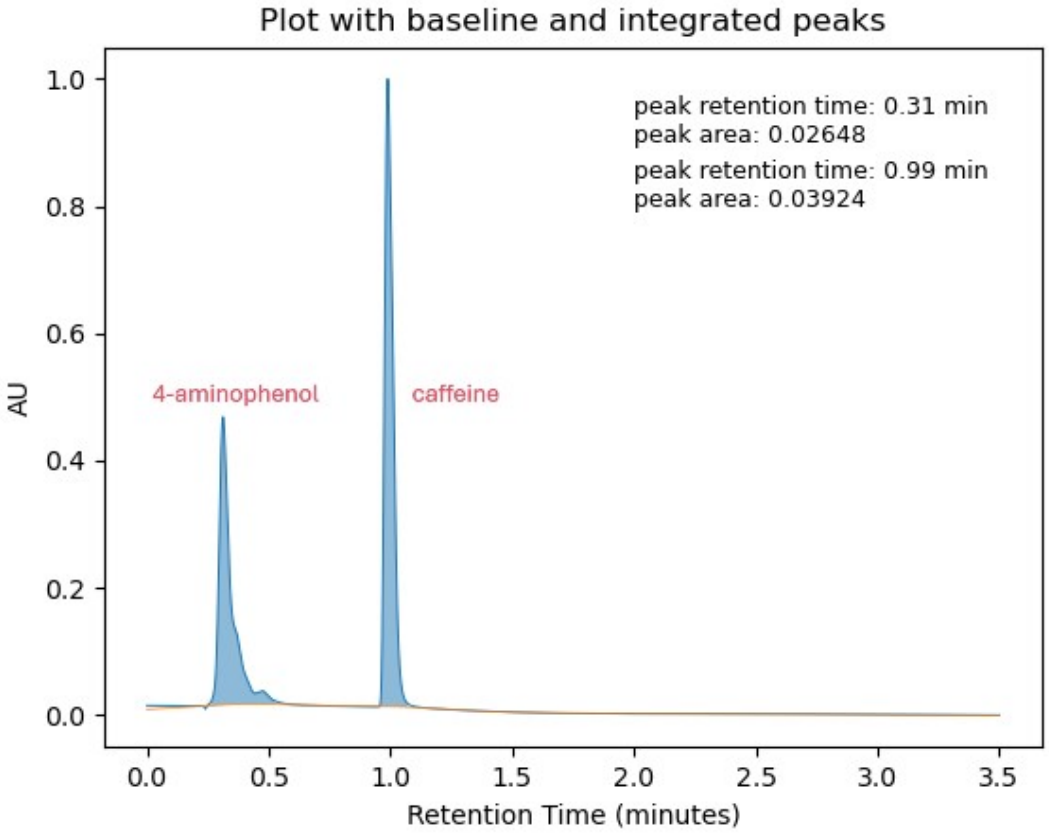

Fig. S22.

08/08/2024 - 14:43:47 – Experiment 1 – Before acetic anhydride addition

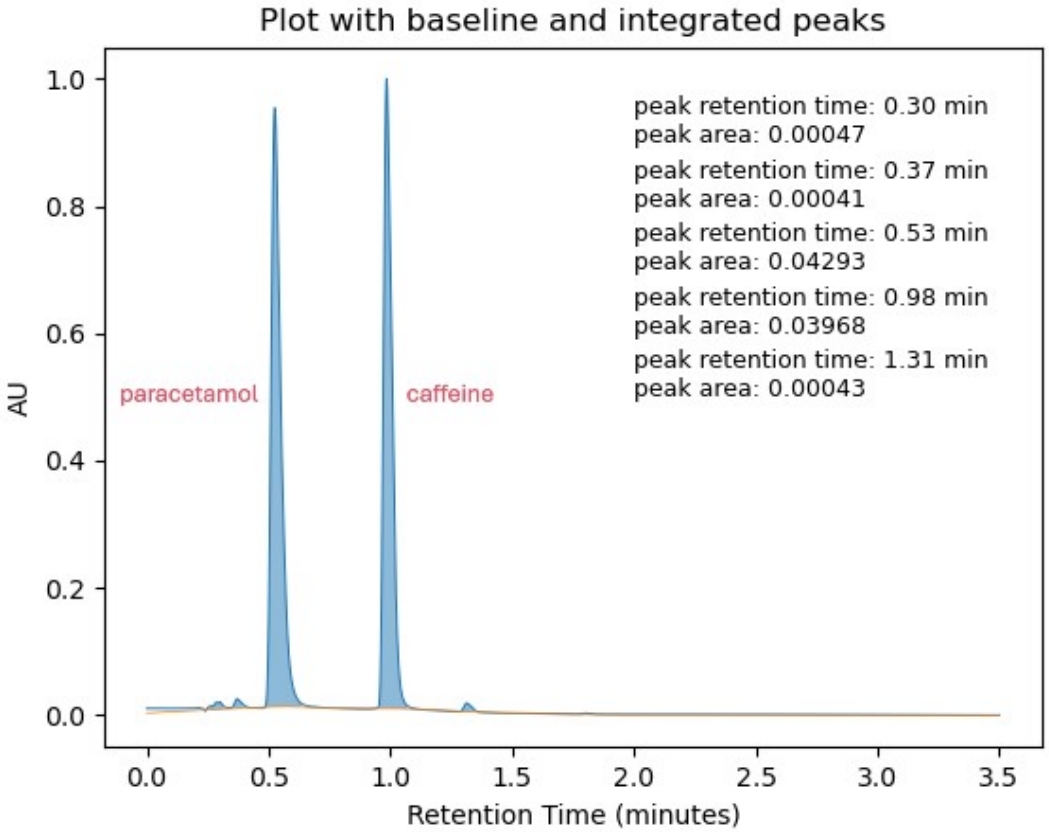

Fig. S23.

08/08/2024 - 15:33:04 – Experiment 1 – After acetic anhydride addition

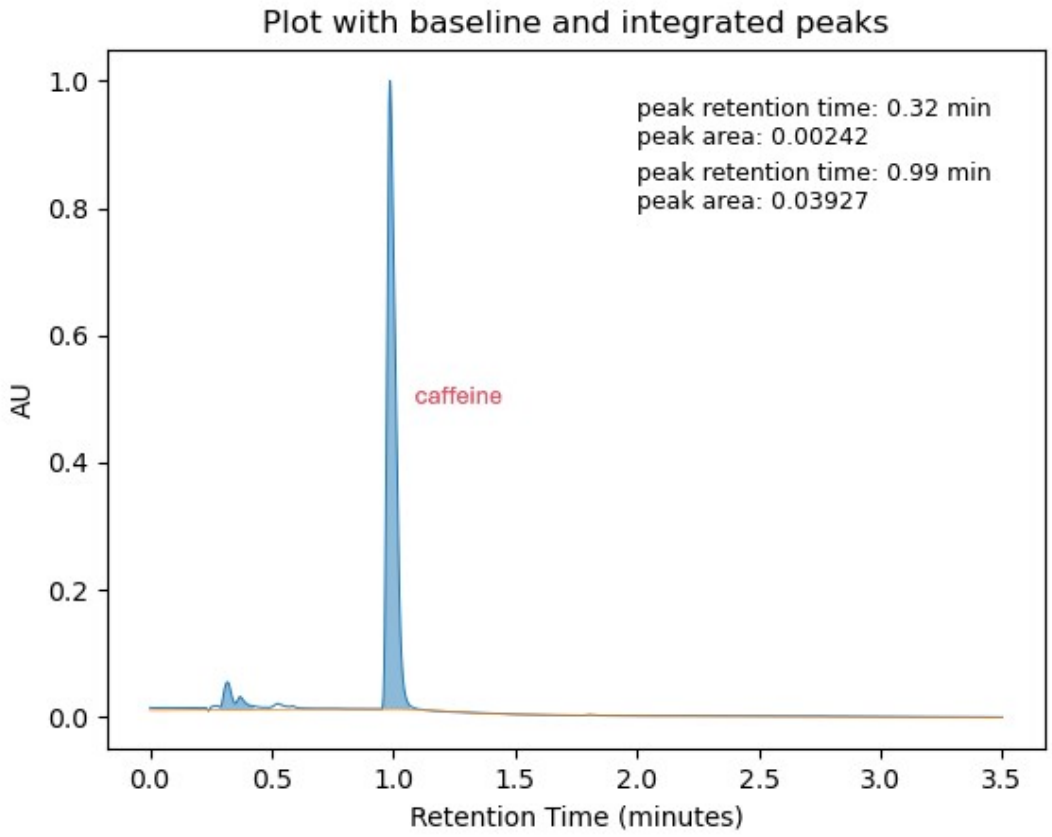

Fig. S24.

08/08/2024 - 18:18:51 – Experiment 1 – Cleaning sample 1

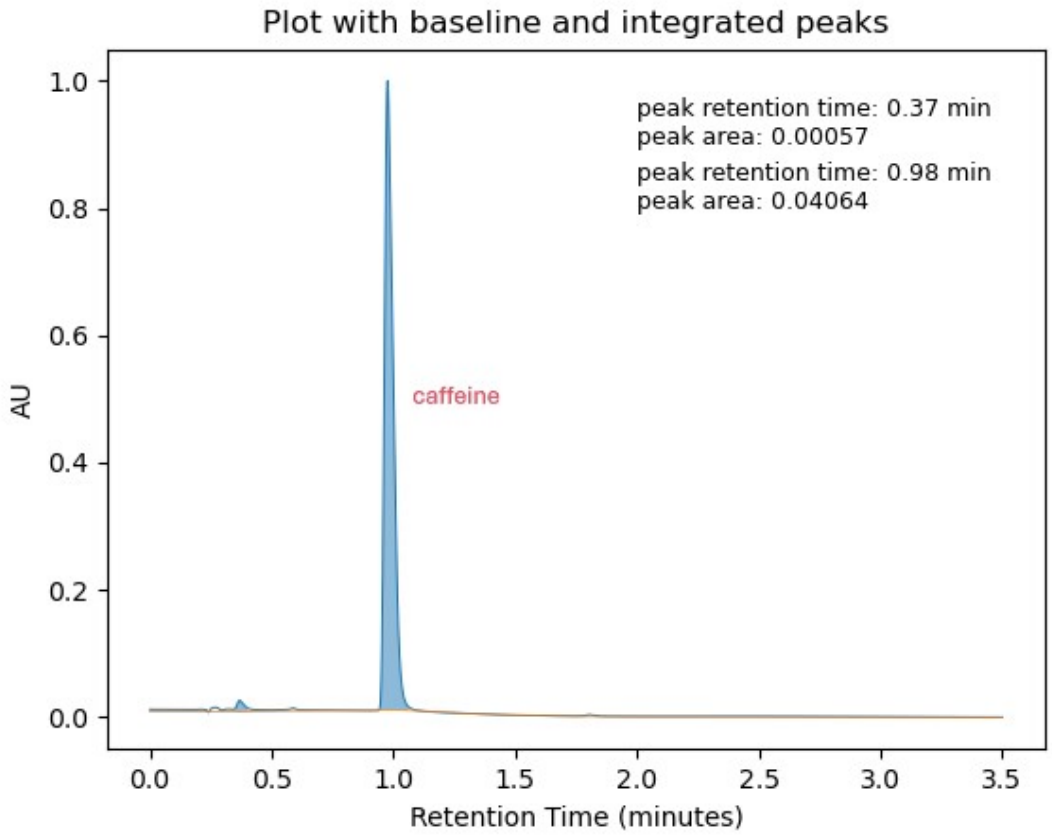

Fig. S25.

08/08/2024 - 19:43:51 – Experiment 1 – Cleaning sample 2

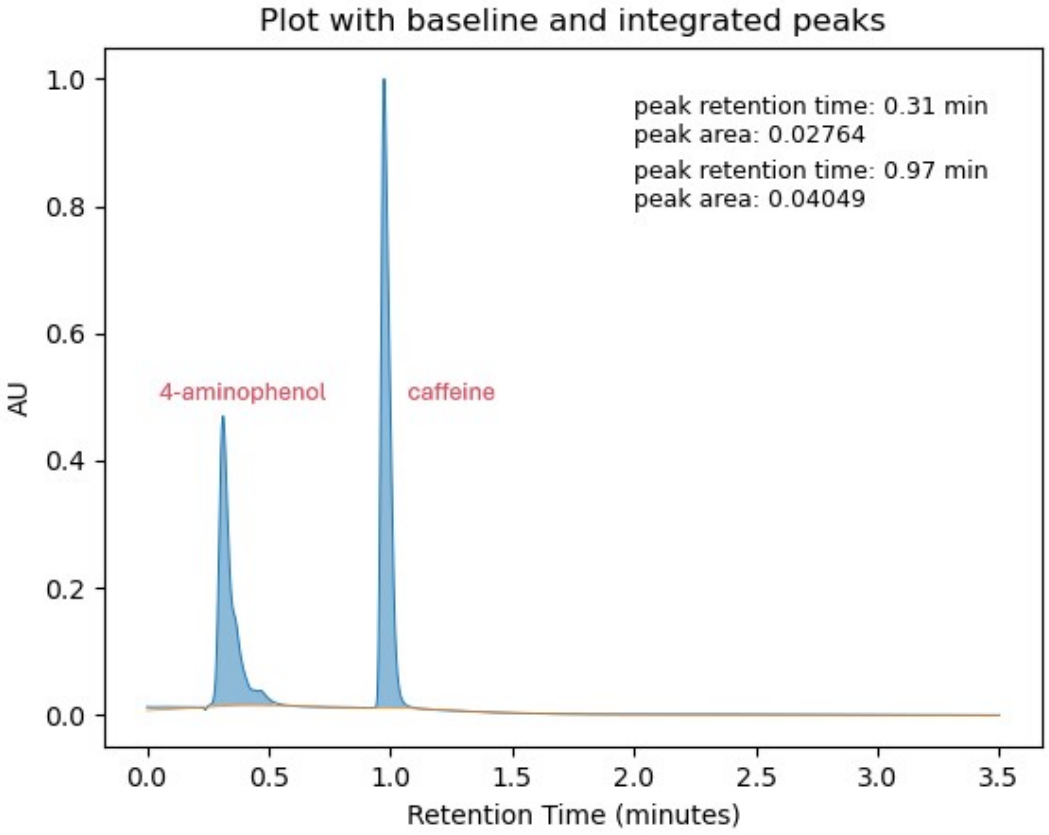

Fig. S26.

08/08/2024 - 21:27:43 – Experiment 2 – Before acetic anhydride addition

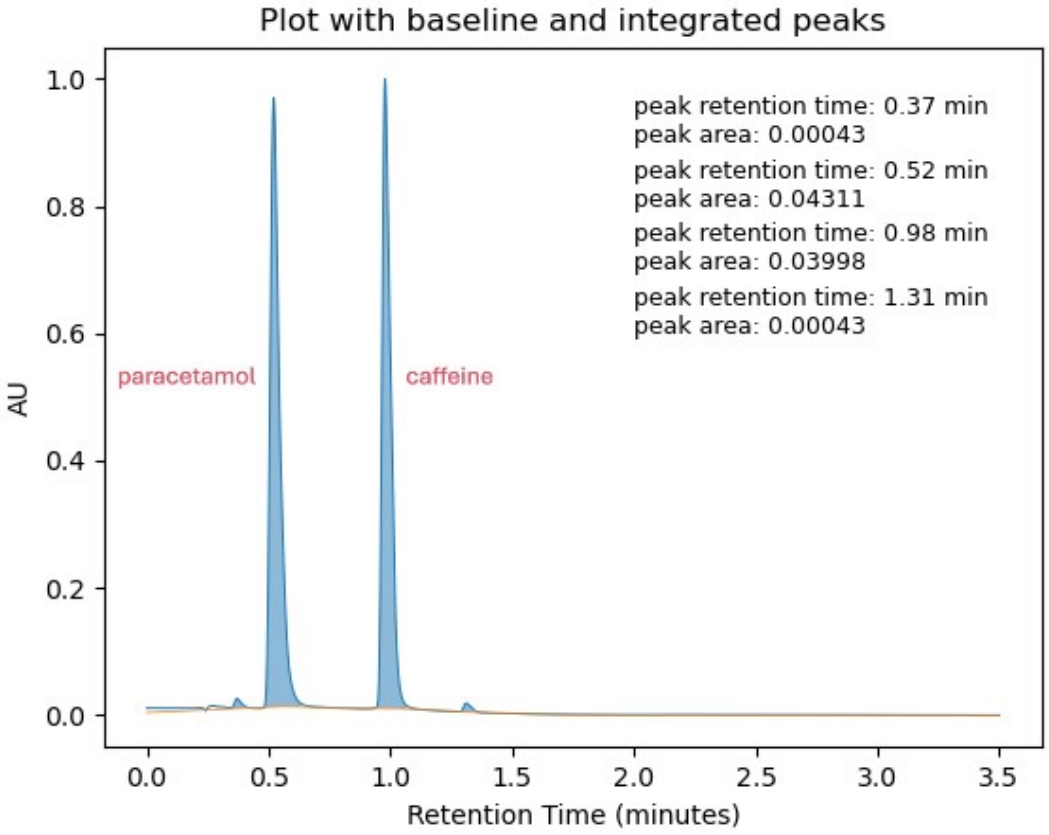

Fig. S27.

08/08/2024 - 22:24:00 – Experiment 2 – After acetic anhydride addition

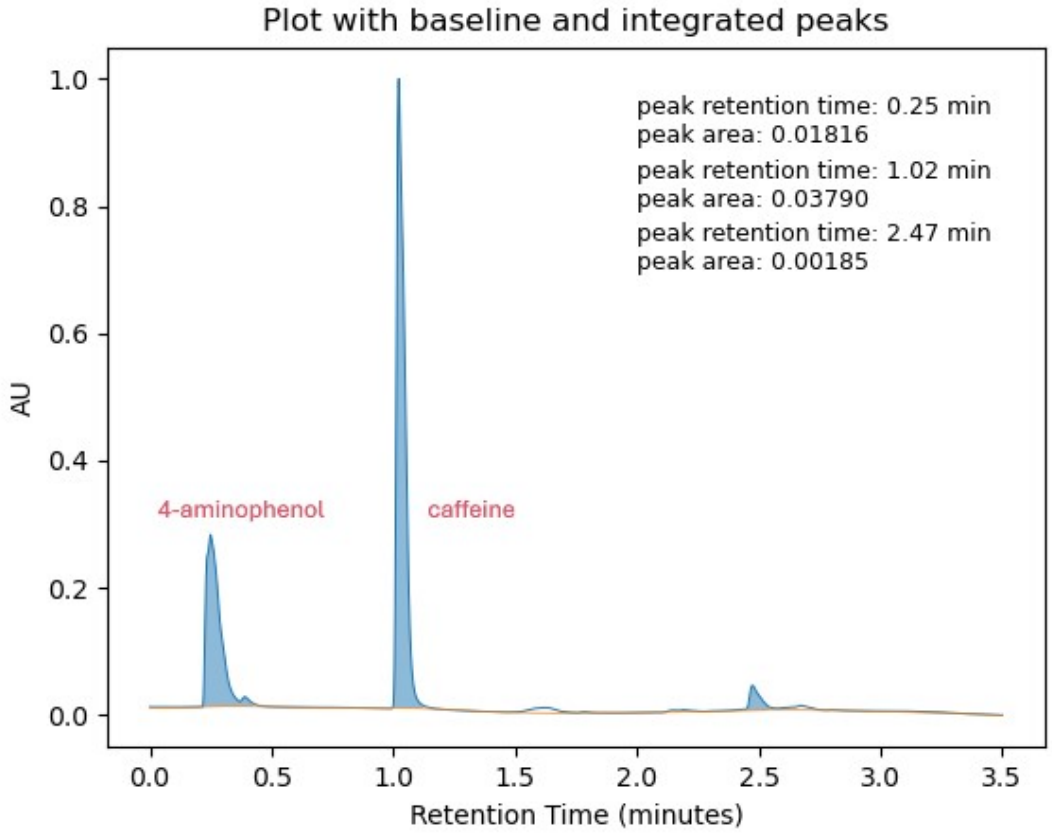

Fig. S28.

28/08/2024 - 12:34:14 – Experiment 1 – Before acetic anhydride addition

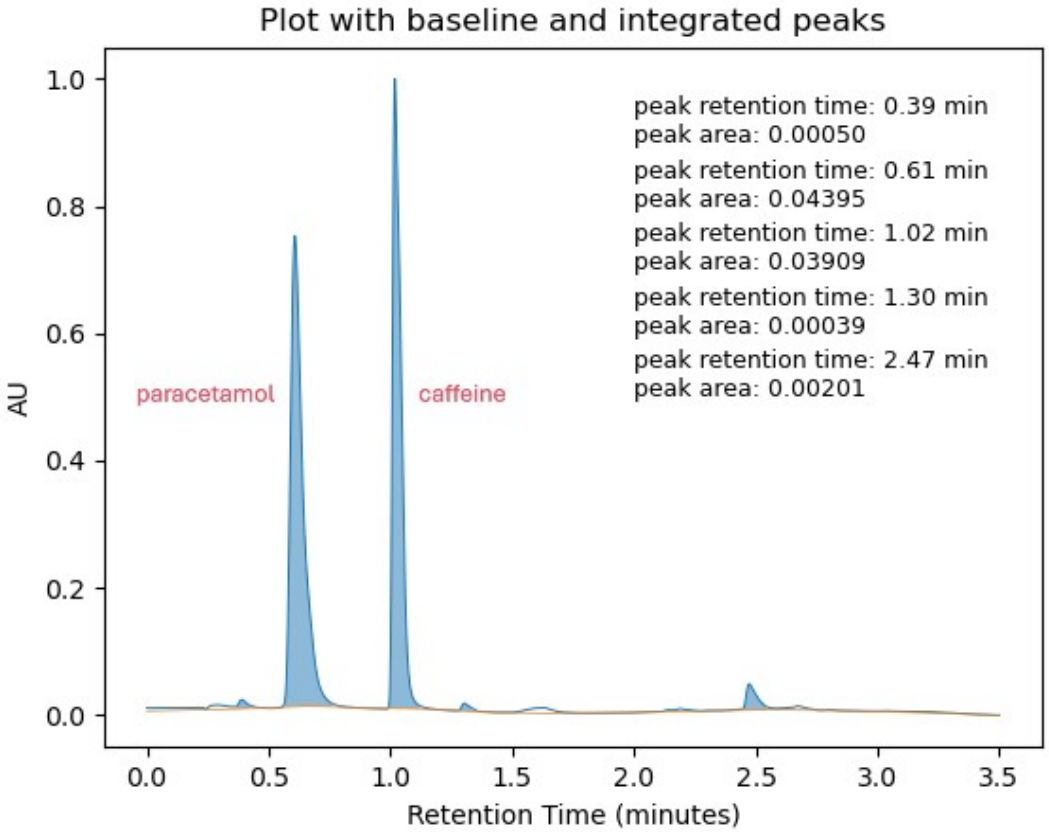

Fig. S29.

28/08/2024 - 13:22:26 – Experiment 1 – After acetic anhydride addition

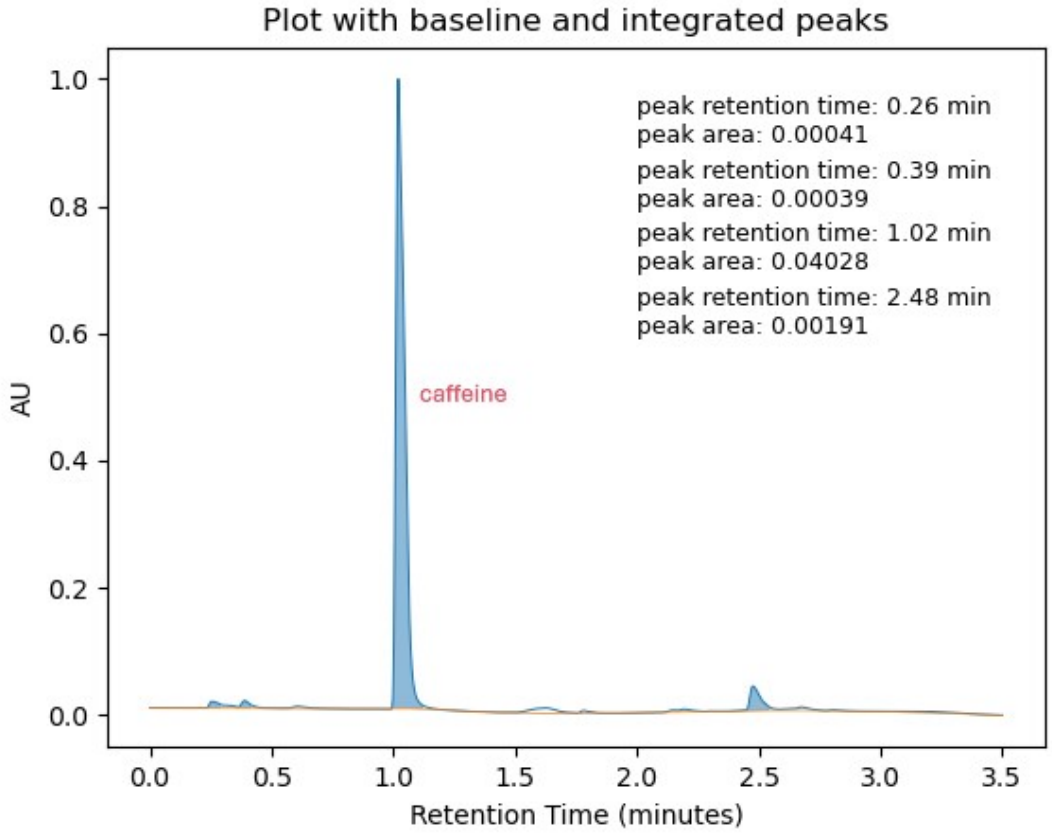

Fig. S30.

28/08/2024 - 16:15:04 – Experiment 1 – Cleaning sample 1

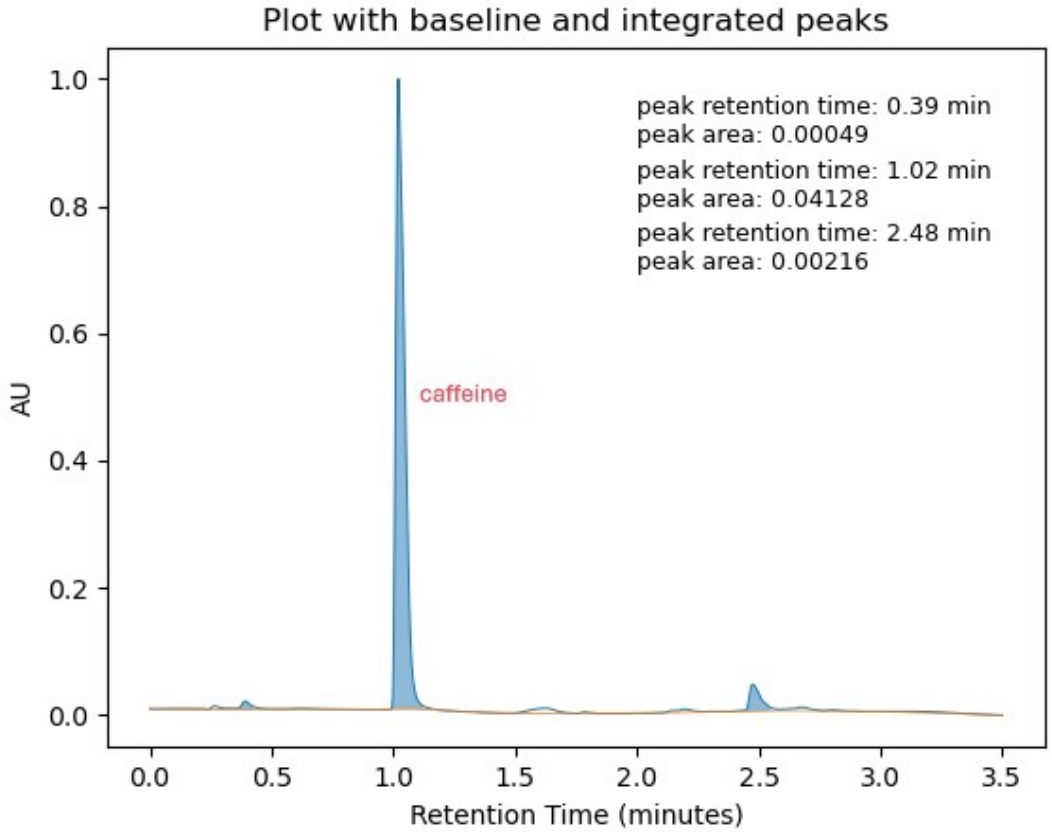

Fig. S31.

28/08/2024 - 17:38:30 – Experiment 1 – Cleaning sample 2

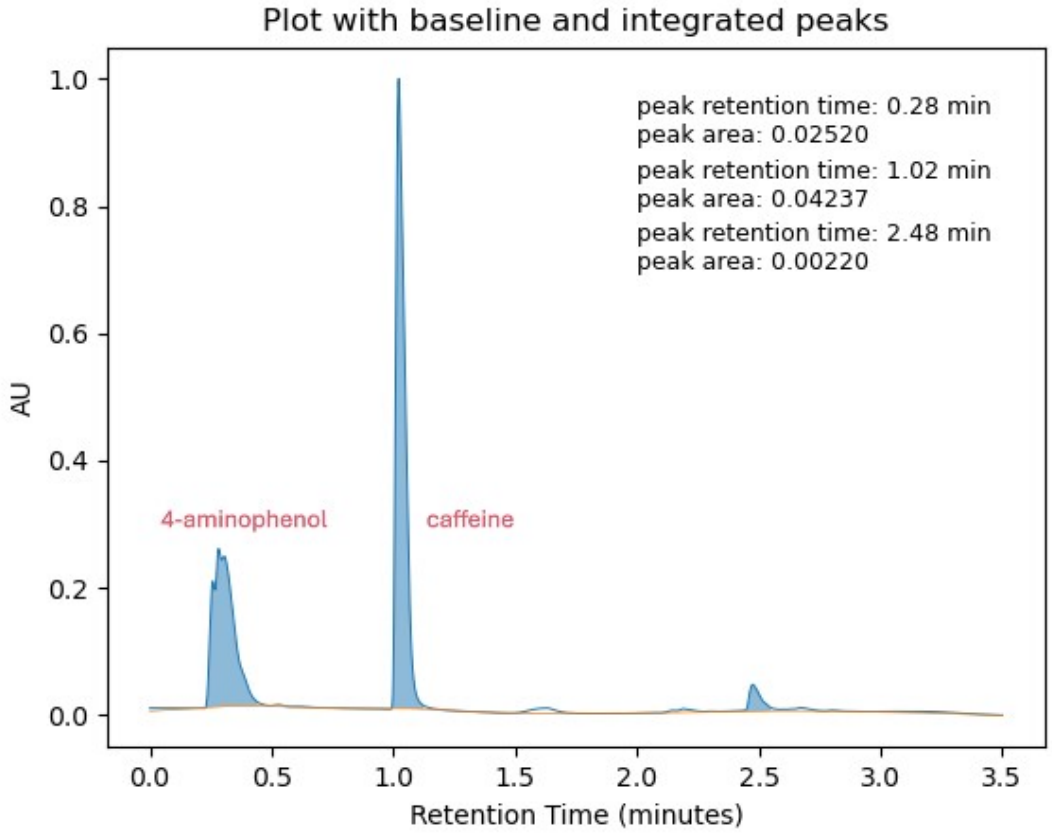

Fig. S32.

28/08/2024 - 19:27:13 – Experiment 2 – Before acetic anhydride addition

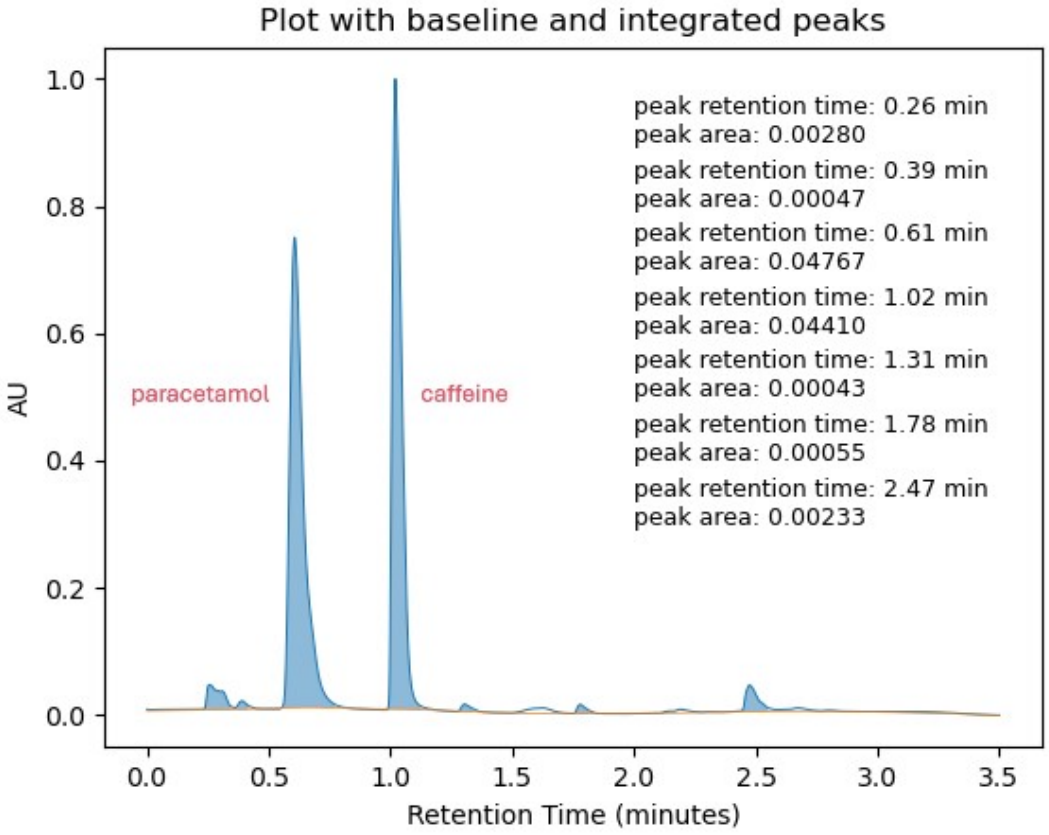

Fig. S33.

28/08/2024 - 20:17:21 – Experiment 2 – After acetic anhydride addition

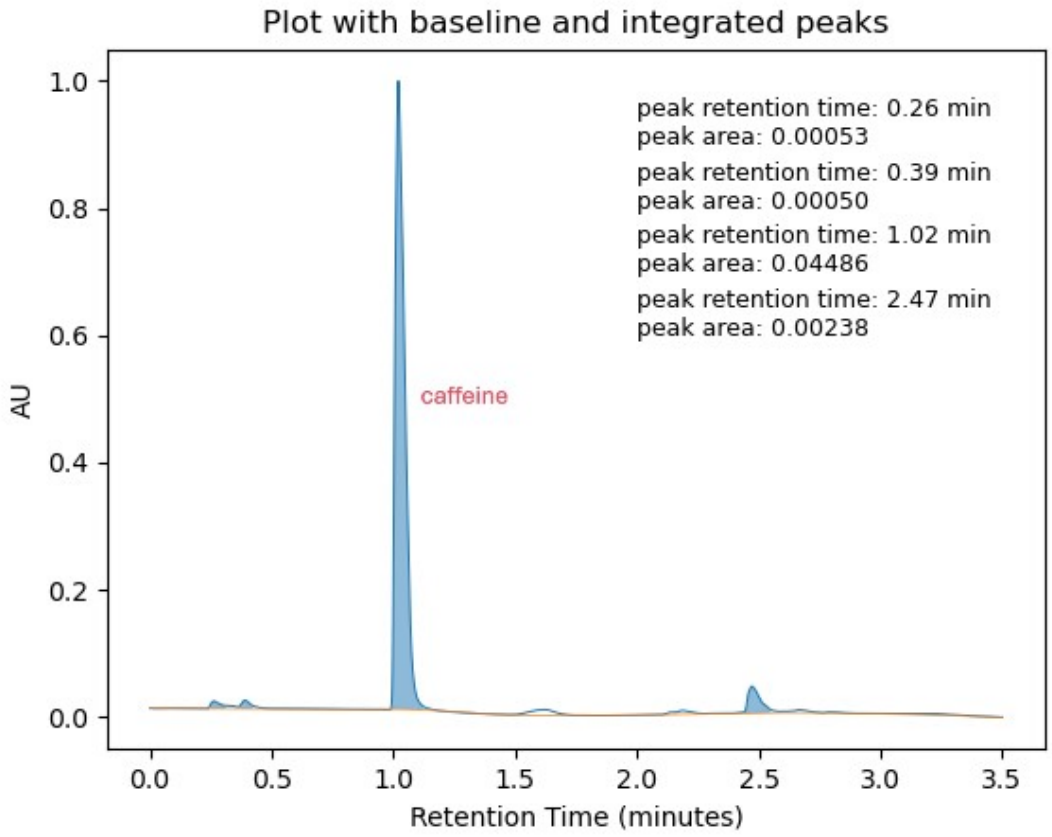

Fig. S34.

28/08/2024 - 23:05:31 – Experiment 2 – Cleaning sample 1

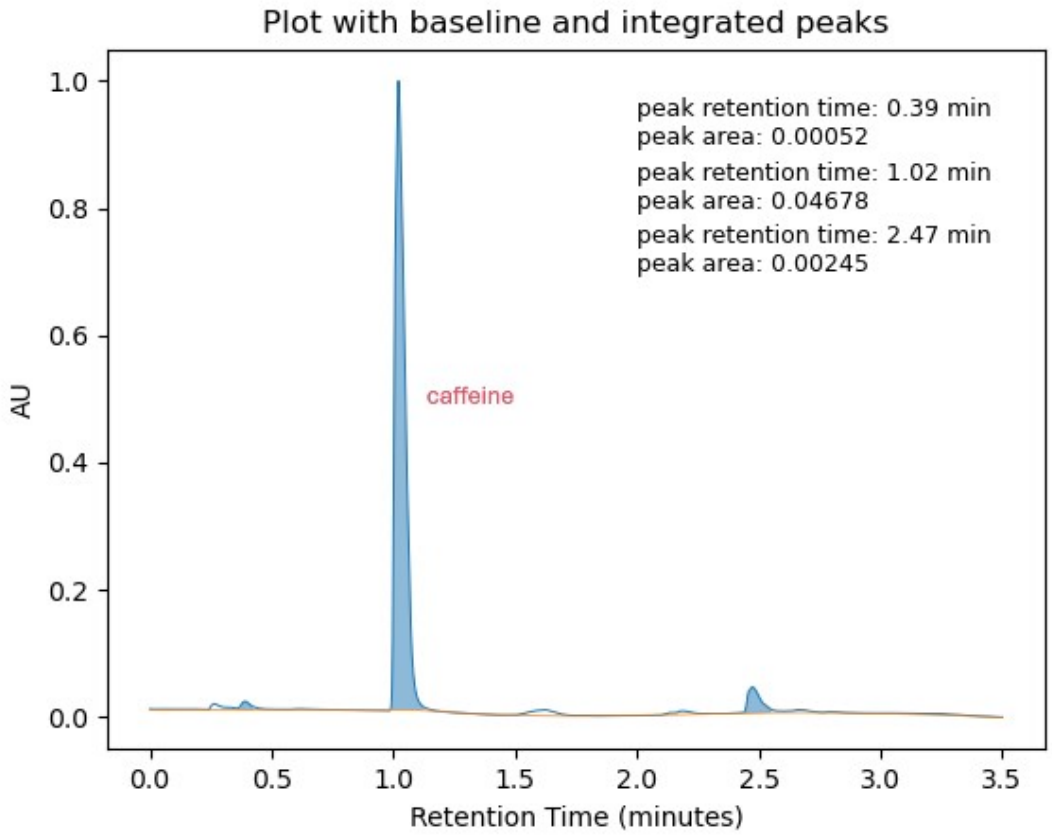

Fig. S35.

29/08/2024 - 00:26:52 – Experiment 2 – Cleaning sample 2

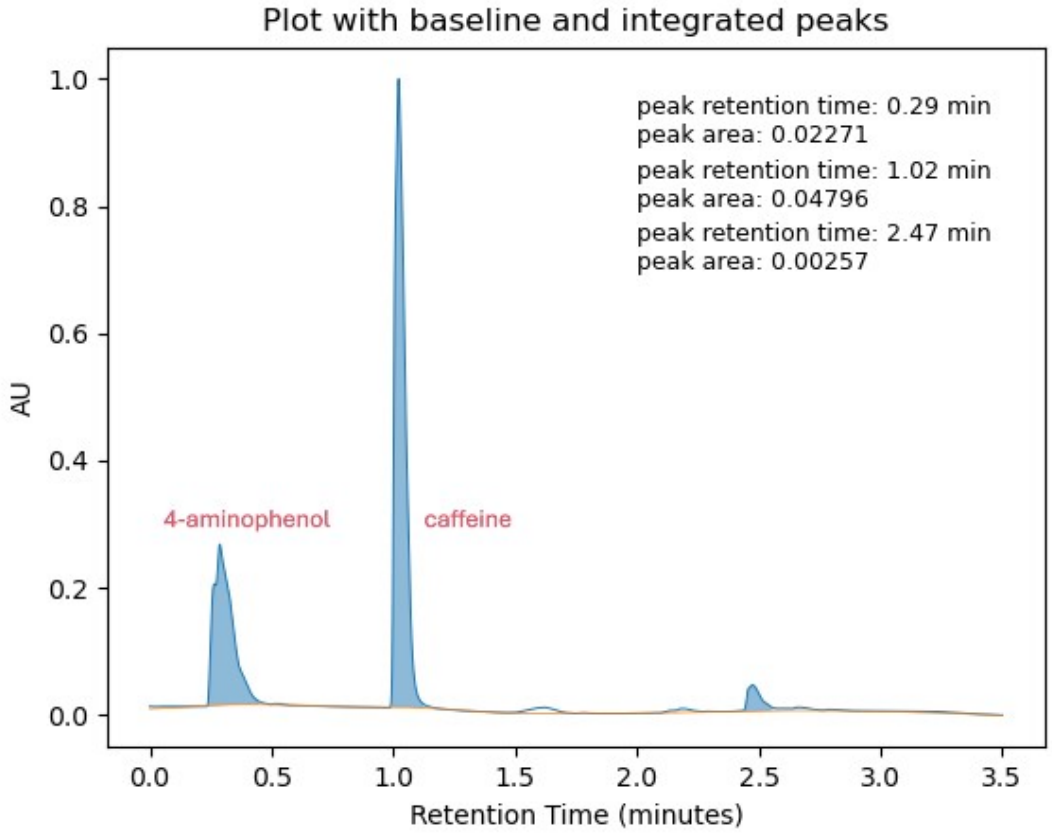

Fig. S36.

29/08/2024 - 02:11:14 – Experiment 3 – Before acetic anhydride addition

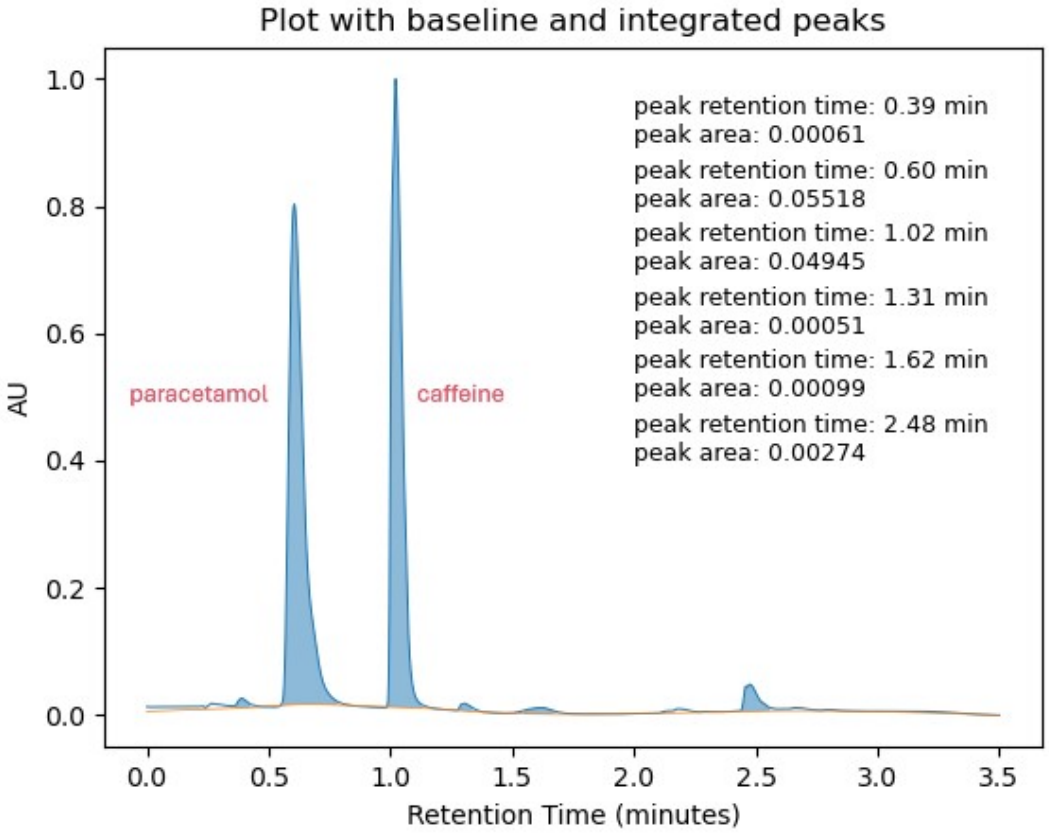

Fig. S37.

29/08/2024 - 03:00:14 – Experiment 3 – After acetic anhydride addition

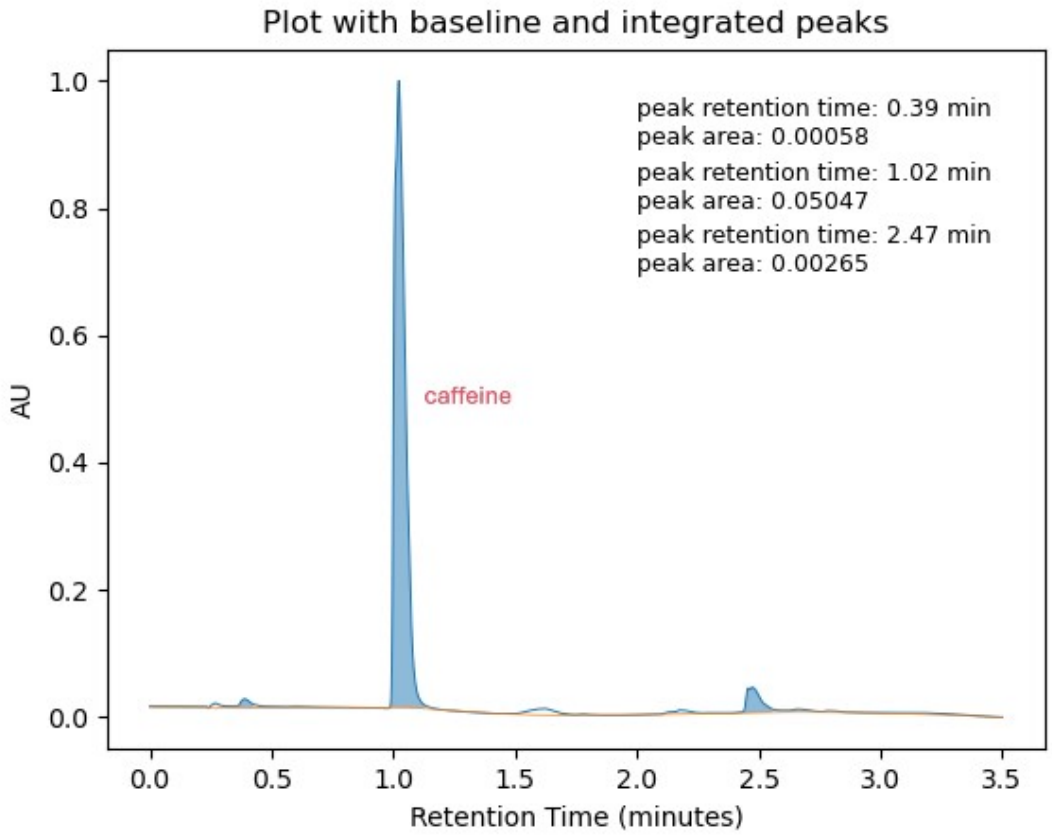

Fig. S38.

29/08/2024 - 06:13:34 – Experiment 3 – Cleaning sample 1

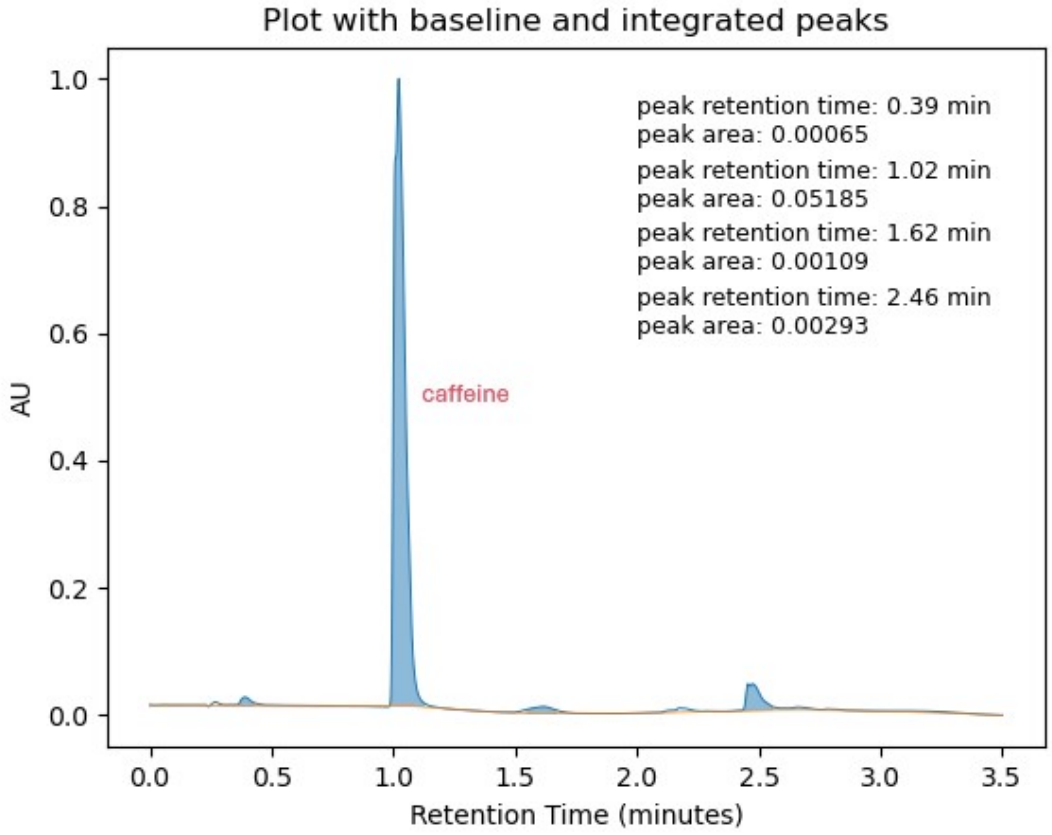

Fig. S39.

29/08/2024 - 07:41:44 – Experiment 3 – Cleaning sample 2

Table S1.

Yields from three successive experiments on August 28th 2024.

Experiment Date - Number	Product Weight (g)	Yield (%)
28/08/24 - 1	15.80	57.0
28/08/24 - 2	15.72	56.8
28/08/24 - 3	15.80	57.0

Table S2.

Yields from preliminary experiments.

Experiment Date - Number	Product Weight (g)	Yield (%)
17/01/24 - 1	14.26	53.0
18/01/24 - 1	13.23	52.8
18/01/24 - 2	14.31	49.0
05/08/2024 - 1	16.32	58.9
08/08/2024 - 1	16.29	58.8

Table S3.

Solid dispensing device testing data; 'mass lost' is undispensed solid remaining in the device.

Mass loaded (g)	Mass dispensed (g)	Mass lost (g)	% (mass lost/mass loaded)
20.05	19.98	0.07	0.35
19.98	19.90	0.08	0.40
20.10	20.02	0.08	0.40
20.00	19.92	0.08	0.40
19.92	19.87	0.05	0.25
19.98	19.93	0.05	0.25
20.03	19.98	0.05	0.25
19.98	19.94	0.04	0.20
19.94	19.91	0.03	0.15
20.06	20.02	0.04	0.20
20.02	19.99	0.03	0.15
19.99	19.96	0.03	0.15
19.96	19.90	0.06	0.30
20.04	19.98	0.06	0.30
19.98	19.96	0.02	0.10
19.96	19.92	0.04	0.20
20.11	20.09	0.02	0.10
20.09	20.04	0.05	0.25
20.04	19.97	0.07	0.35
19.97	19.92	0.05	0.25

Table S4.

Full data for the sample taken after acetic anhydride addition in each experiment.

Experiment Date - Number	Paracetamol peak area	Caffeine peak area	Paracetamol/caffeine peak area ratio	Calculated paracetamol concentration (mg/mL)
17/01/2024 - 1	0.03359	0.03243	1.036	0.4901
17/01/2024 - 2	0.03188	0.02998	1.063	0.5032
18/01/2024 - 1	0.02943	0.02938	1.002	0.4740
18/01/2024 - 2	0.02838	0.03081	0.9211	0.4359
05/08/2024 - 1	0.04420	0.03984	1.109	0.5250
08/08/2024 - 1	0.04293	0.03968	1.082	0.5119
08/08/2024 - 2	0.04311	0.03998	1.078	0.5102
28/08/2024 - 1	0.04395	0.03909	1.124	0.5320
28/08/2024 - 2	0.04767	0.04410	1.081	0.5115
28/08/2024 - 3	0.05518	0.04945	1.116	0.5280

Movie S1.

An edited video demonstrating one automated paracetamol synthesis experiment, showing details in individual steps. The following narrative describes the various workflow steps and relevant timestamps in the video. Total timescale for experiment = 6 h 54 m.
This video is available to view on YouTube at the following URL:
https://www.youtube.com/watch?v=XdxzEjBgC0Q

Timestamps:
00:00 – 00:08: Introduction.
00:09 – 00:30: Robot moves funnel from storage shelf to filtration system.
00:31 – 00:35: 500 mL of water dispensed into reactor.
00:36 – 01:17: 20 g of 4-aminophenol dispensed into reactor.
01:18 – 01:33: Reactor heated to 700 ºC, stirred at 400 rpm.
01:34 – 01:57: Autosampler takes sample from reactor and robot collects sample.
01:58 – 01:59: 35 mL of acetic anhydride dispensed into reactor.
02:00 – 02:38: Robot moves sample to UHPLC-MS machine; analysis runs.
02:39 – 02:41: Robot arm calibrates.
02:42 – 03:26: Robot takes second sample to UHPLC-MS machine; analysis runs.
03:27 – 03:30: 30 minutes wait for crystallisation cooling to 5 ºC.
03:31 – 03:41: Filtration begins.
03:42 – 03:47: Reactor refilled with 600 mL water.
03:48 – 04:02: Filtration continues.
04:03 – 04:04: Drying.
04:05 – 04:23: Funnel weighed and returned to storage shelf.
04:24 – 04:32: Hollow funnel loaded onto filtration system.
04:32 – 04:37: Reactor filled with 600 mL distilled water.
04:38 – 04:43: Reactor heated to 85 ºC, stirred at 400 rpm.
04:44 – 04:47: Robot arm calibrates.
04:48 – 04:51: Reactor continues heating to 85 ºC.
04:52 – 05:11: First cleaning sample taken to UHPLC-MS machine; analysis runs.
05:12 – 05:14: Water drained from reactor.
05:15 – 05:20: Reactor filled with 600 mL distilled water again.
05:21 – 05:27: Reactor heated to 85 ºC and stirred at 400 rpm.
05:28 – 05:44: Second cleaning sample taken to UHPLC-MS machine; analysis runs.
05:45 – 05:52: Robot charges.
05:53 – 06:00: Second cleaning sample unloaded from UHPLC-MS machine.
06:01 – 06:03: Water drained from reactor.
06:04 – 06:26: Robot moves back to fume hood and returns hollow funnel to base.
06:26 – 06:31: System is ready for the next experiment.

Movie S2.

Raw, unbroken footage demonstrating the automated workflow running over the course of 21 hours—that is, three back to back automated experiments—sped up x100. The narrative below describes the various workflow steps and relevant timestamps in the video. Timestamps refer to the accelerated video (min:sec), not the chronological time in the experiment. Note that from this fixed camera perspective, the UHPLC-MS operations (which is behind the fumehoods) cannot be seen; see edited Movie 1 for those details, as well as close ups of individual operations.

This video is available to view on YouTube at the following URL:
https://www.youtube.com/watch?v=Pvdyf3zxtlk

Timestamps:
00:00 – 04:09: Experiment 1
Synthesis and analysis
00:00 – 00:03: Robot moves funnel from storage shelf to filtration system.
00:04 – 00:09: 500 mL of water dispensed into reactor.
00:10 – 00:16: 20 g of 4-aminophenol dispensed into reactor.
00:17 – 00:31: Reactor heated to 70 ºC, stirred at 400 rpm.
00:32 – 00:34: Autosampler takes sample from reactor and robot collects sample.
00:35 – 01:00: Robot moves sample to UHPLC-MS machine; analysis runs.
01:01 – 01:18: Robot takes second sample to UHPLC-MS machine; analysis runs.
01:19 – 01:20: Robot arm calibrates.
01:21 – 01:28: UHPLC-MS analysis continues, robot collects sample.
01:29 – 01:51: 30 minutes wait for crystallization cooling to 5 ºC.
Filtration, drying & product weighing
01:52 – 02:07: Filtration and drying.
02:08 – 02:16: Funnel weighed and returned to storage shelf.
02:17 – 02:19: Hollow funnel loaded onto filtration system.
02:21 – 02:25: Chemist reloads first solid dispensing cartridge.
Reactor cleaning for next run
02:26 – 02:43: Reactor filled with 600 mL water, heated to 85 ºC, stirred at 400 rpm.
02:44 – 02:53: First cleaning sample taken to UHPLC-MS machine; analysis runs.
02:54 – 02:55: Robot arm calibrates.
02:56 – 03:05: UHPLC-MS analysis continues, robot collects sample.
03:06 – 03:34: Water drained, reactor refilled with 600 mL water, heated to 85 ºC, stirred at 400 rpm.
03:35 – 03:44: Second cleaning sample taken to UHPLC-MS machine; analysis runs.
03:35 – 03:57: Robot charges.
03:58 – 04:03: UHPLC-MS analysis continues, robot collects analysis sample.04:04 – 04:09: Robot moves back to fume hood and returns hollow funnel to base.
04:10 – 08:11: Experiment 2 (repeat of above)
08:12 – 12:31: Experiment 3 (repeat of above)